The development of a clinically applicable growth factor-releasing biomaterial to promote endogenous stem cell repair of the brain after stroke

Tongda Li

Thesis submitted to the University of Ottawa

in partial Fulfillment of the requirements for the degree of

MASTER OF APPLIED SCIENCE

in Chemical Engineering

Department of Chemical and Biological Engineering

Faculty of Engineering

University of Ottawa

Abstract

Endogenous neural stem/progenitor cells therapy is one of the most advanced clinical trial worldwide. Generally, drug is given to the targeted area through the traditional strategies such as intraventricular or intravenous delivery method. However, those methods always come with undesired side-effects such as over-dose of drug and offensive injection are not applicable to the large-scale clinical application. In this study, the clinical feasibility of blended biosynthesized cellulose duraplasty was studied. Our results showed that physical properties of BBC can be controlled through the optimized fabrication process. In addition, the time length of Middle cerebral artery occlusion rat model was tested through the 60 vs 90 mins occlusion time behavioral assessments of rat and the data indicated that 60 mins length can induce significant motor functional impairment. Finally, the EGF & EPO-loaded BBC duraplasty was implanted over the removed area and the ELISA test revealed that BBC duraplasty can release and delivery the growth factors to the targeted area (subvertical zone) at lease 3 days after implantation. In summary, our BBC duraplasty is showing the potential prospection to be a clinical-applicable duraplasty to replace the traditional commercial duraplasty in the future stroke recovery therapy.

Keywords: stroke; duraplasty; endogenous stem cells; growth factors; rodent model; blended biosynthesized cellulose

Abstrait

La thérapie des cellules souches neurales endogènes/cellules souches progéniteurs est l'une des essais cliniques les plus avancés au monde. Généralement, le médicament est offert à la zone ciblée par le biais des stratégies traditionnelles telles que les méthodes de distribution intraventriculaire ou intraveineuse. Cependant, ces méthodes s'accompagnent toujours par des effets secondaires indésirables, tels qu'une surdose du médicament et l'injection offensive, et ne sont pas applicables à une application clinique à grande échelle. Dans cette étude, la faisabilité clinique du duroplastie en cellulose biosynthérisée mixte a été étudiée. Nos résultats ont démontré que les propriétés physiques du BBC peuvent être contrôlées à travers le processus de fabrication optimisé. En addition, la durée du modèle d'occlusion de l'artère cérébrale centrale chez le rat a été testé à travers des évaluations comportementales du temps d'occlusion de 60 versus 90 minutes du rat et les données ont indiqué qu'une longueur de 60 minutes peut induire une déficience fonctionnelle motrice importante. Finalement, la duroplastie BBC chargée d'EFG et d'EPO a été implanté sur la zone retirée et le test ELISA a révélé que la duroplastie BBC peut libérer et délivrer les facteurs de croissance à la zone ciblée (zone subverticale) au moins 3 jours après l'implantation. En résumé, notre duroplastie BBC montre la perspective potentielle de devenir une duroplastie applicable en clinique afin de remplacer la duroplastie commerciale traditionnelle dans les traitements futurs de la récupération de l'accident vasculaire cérébral.

Mots-clés: accident vasculaire cérébral; duroplastie; cellules souches endogènes; facteurs de croissance; modèle de rongeurs; cellulose biosynthérisée mixte

Statement of originality

The content presented in this document is the product of original work performed by the author at the University of Ottawa under the supervision of Professor Xudong Cao

In partial fulfillment of the requirements for the degree of Master of Science (Chemical Engineering) at the University of Ottawa, this work was presented at the University of Ottawa for the Chemical Engineering graduate student seminar:

Tongda Li, Xudong Cao, Eve Tsai. The development of a clinically applicable growth factor-releasing biomaterial to promote endogenous stem cell repair of the brain after stroke. University of Ottawa for Department of Chemical Engineering, October 2019.

A poster on the similar topic was presented at the Neurotrauma 2018 Conference:

Tongda Li, Ryan V. Sandarage, Taisa R. Stumpf, Suzan Chen, Auriat Angela, Eve Tsai, Xudong Cao. Efficacy of a dura-plasty biomaterial to promote neural stem cell proliferation after traumatic brain injury

Statement of contribution

The entirety of this document was written by the author. All figures and tables were created by the author unless otherwise mentioned in the caption

The work presented was largely performed by the author including fabrication and characterization of the duraplasty. The blank BBC membranes were designed and initially characterized by Dr. Taisa R. Stumpf. The stroke model was partially performed by Dr. Angela Auriat and Dr. Zhiwen Su. The behavioral assessment was partially performed by Ms. Charlotte Meneghin.

Acknowledgements

First, I would like to thank my supervisor Dr. Xudong Cao for his consistent support through-out this journey. I am very grateful for the opportunities that he has provided and for his enthusiasm about the project.

Second, I would like to thank Dr. Eve Tsai for her patience and motivation as my co-supervisor. I would also like to thank Dr. Suzan Chen, Dr. Angela Auriat and Dr.Su for all their help with this work as well as the other members of my lab for being so kind and providing moral support.

Third, I would like to thank my family and friends. Thank you for always encouraging and believing in me.

Table of content

List of Abbreviations

ATCC	American Type Culture Collection
BBB	Blood-brain barrier
BBC	Blended biosynthesized cellulose
BC	Biosynthesized cellulose
BCF	Bacterial cellulose nanofiber
BC-HA	Bacterial cellulose-hydroxyapatite
BCM	Bacteria cellulose membranes
BDNF	Brain-derived neurotrophic factor
BMP-2	Bone morphogenetic protein-2
BNC	Bacterial nanocellulose
BSA	Bovine serum albumin
CBF	Cerebral blood flow
CFU	Colony-forming unit
CNS	Central nervous system
CSF	Cerebrospinal fluid
CVI	Cerebrovascular insult
DC	Decompressive Craniectomy
ECM	Extracellular matrix
EGF	Epidermal growth factor
EPO	Erythropoietin
eNSPCs	Endogenous neural stem/progenitor cells
ET-1	Endothelin-1
FDA	Food & Drug Administration
FGF-2	Fibroblast growth facor-2
HAMC	Hyaluronan-methylcellulose
HAP-DN	Hydroxyapatite double-network
HASCs	Human adipose-derived mesenchymal stem cells
hNT	Human NT2N
HUVEC	Human vein endothelial cells
ICA	Internal cerebral artery
IGF1	Insulin-like growth factor-1
IV	Intravenous therapy
MCAo	Middle cerebral artery occlusion
MSCs	Mesenchymal stem cells
NSC	Neural stem cells
OCT	Optimal cutting temperature
PFA	Paraformaldehyde
PLLA	Polylactic acid
PTFE	Polytetrafluoroethylene
PVA	Polyvinyl alcohol
SAH	Subarachnoid hemorrhage
SEM	Scanning electronic microscope

SR	Swelling ratio
SVZ	Subventricular zone
TE	Tissue engineering
tPA	Tissue plasminogen activator
VEGF	Vascular endothelial growth factor
mNSS	Modified Neurological Severity Scores

List of Tables

List of Figures

1. Introduction

It is well known that stroke can lead to long-term adult disability.[1]. 90% of stoke survivors are suffering from the functional impairment[2]. Even though the systemic thrombolytic therapy such as tissue plasminogen activator (tPA) is an effective treatment to save patient's life, the limitation of tPA is obvious due to the fact that the treatment window is only 4.5 hours after the onset of the stroke and it is not a recovery treatment hence cannot promote the stroke rehabilitation[3-8]. In addition, most of traditional treatment options such as oral administration and intravenous injection are limited because of the blood-brain barrier (BBB) and hence it is difficult for therapeutic drugs pass through the BBB in order to be effective for the stroke patients [9-12].

To date, stem cell therapy is one of the most promising strategies in the stroke recovery. Generally, exogenous and endogenous stem cell treatments are the two main categories of stem cell therapies[13]. Because of the concern of ethical issue and undesirable immune reaction, the exogenous stem cell therapy cannot be deemed an ideal candidate to the stroke treatment[14]. Therefore, the discovery of patient's own stem cell became a better option for the stroke recovery. Recently, endogenous neural stem/progenitor cells (eNSPCs) have been stimulated by several methods to achieve differentiation to determine if it can repair the brain issue after stroke [12, 15-18] . It is an attractive therapeutic option as the transplantation of stem cells is not required and hence ethical concern and foreign rejection associated with the exogenous stem cells from other sources is avoided. However, the main limitation of endogenous strategies is obvious since regeneration are often not sufficient for the structural or functional reestablishment of the injured brain[19]. Until now, one of the current approaches to deal with this dilemma is to deliver the growth factors which significantly increase the eNSPCs survival rate (i.e. up to 100-fold) and has

been shown to restore motor function in various animal models of stroke[20-23]. Generally, growth factors are typically administrated via an invasive-ventricular pump or intraparenchymal injection such as injectable hydrogel[24-30]. For example, Carmichael and Cook *et al*. injected hydrogel incorporating Brain-derived neurotrophic factor (BDNF) to the stroke cavity on mice stroke model, and the results showed that the hydrogel-delivered BDNF induced significant improvement of neurogenesis after stroke compare to the control group. Coincidentally, Etgen and Traub lab introduced insulin-like growth factor-1 (IGF1) through the intracerebroventricular cannula on adult female rats that underwent four vessel global ischemia surgeries, and the authors demonstrated that the amount of surviving cornu Ammonis 1 (CA1) pyramidal neurons of IGF1 treatment group was higher than the control group. However, those invasive methods also bring with undesirable side-effect. [31]. For example, injection of additional material into a already edematous brain during the early stages of stroke could potentially precipitate death due to the increased mass effect with brain herniation[32-34].Therefore, it is clear that interventricular infusion is not a clinically feasible method to administer these growth factors to the brain.

Decompressive Craniectomy (DC) is a surgical procedure that can reduce mortality through releasing the elevated intracranial pressure caused by the stroke[35, 36]. After the removal of the part of skull, a duraplasty is usually used to replace dura mater as a protective layer on the surface of the brain to avoid cerebrospinal fluid (CSF) leakage and surgical site infections as well as meningitis. However, DC and duraplasty itself, do not enhance any improvement in neurological recovery. Therefore, we propose to utilize a novel duraplasty material that can be used during the DC procedure for the targeted delivery of growth factors to the injured hemisphere to promote functional recovery after stroke.

The biomaterial we employ to fabricate the duraplasty is biosynthesized cellulose (BC), which has various unique properties, such as biocompatibility, higher crystallinity and excellent purity[36-45]. The structures of BC, such as thickness, homogeneity, and density of the network can be modified to prepare a desired drug delivery system. Recently, several biosynthesized celluloses based drug delivery systems, such as biocellulose composites loaded with biomolecules, nanoparticles and microspheres have been reported[46-48]. For example, biosynthesized cellulose scaffolds loaded with bone morphogenetic protein-2 (BMP-2) have been applied to release BMP-2 for bone tissue engineering (TE). The *in vitro* results show that the BMP-2 loaded scaffolds induce differentiation of mouse fibroblast-like C2C12 cells into osteoblasts and that the osteogenic activity of induced osteoblasts is positively correlated to concentrations of BMP-2 that are used in the scaffolds. However, it is noted that because most therapeutic drugs are incorporated into the BC scaffolds during the scaffold fabrication step, subsequent sterilization step would likely render the incorporated drugs denatured, this is particularly true for protein based growth factors [49-51]. This is perhaps the most likely reason why BC based scaffolds have rarely been used as drug delivery systems for growth factors. In order to solve this issue, we developed a new fabrication procedure. In this study, the novel blended biosynthesized cellulose (BBC) has the potential to replace the current duraplasty and take advantage of the "open" opportunity that is afforded by DC to release the bio-active drugs to stimulate the proliferation and differentiation of eNSPCs after stroke.

The objective of this study is to prepare a growth factor-incorporated duraplasty to enhance neuronal functional recovery after stroke. To achieve this, BBC membranes will be prepared, and their physical properties will be characterized. In addition, as a proof-of-concept, feasibilities of the BBC membranes as duraplasty are investigated in animal studies *in vivo*.

2. Literature Review

2.1 Stroke

Stroke, also known as cerebrovascular insult (CVI), is the sudden death of brain cells due to lack of oxygen and nutrients. Stroke is the second leading cause of death and the third leading cause of disability worldwide[52], with the prevalence of 15 million people suffering from stroke every year. In addition, there is significant financial burden on the stroke patients and the society as a whole [53]. There are two major kinds of strokes: ischemic and hemorrhagic. Ischemic stroke occurs when a vessel supplying brain tissue is blocked. When this happens, the brain cells (neurons) cannot receive enough nutrients and will eventually stop working and die[54]. By contrast, hemorrhagic strokes are less common -- in fact only 15 percent of all strokes are hemorrhagic-- but they are responsible for about 40 percent of all stroke deaths. A hemorrhagic stroke is either a brain aneurysm burst or a weakened blood vessel leak. As a result, blood spills into the brain and creates swelling and pressure[55].

2.1.1 Approach to Overcome Stroke

To date, options to treat stroke are limited and the neurological damage that occurs cannot be recovered[56-58]. Previously, only tPA has been approved by the FDA for acute ischemic stroke, which is given via intravenous therapy (IV) and works by dissolving the clot and improving blood flow[3-5]. Several studies have confirmed the effectiveness of this approach if it is performed within a very restrictive therapeutic window[8, 59-61], which is estimated to be 3 to 4.5 hours from onset of the stroke[62], suggesting that only a small fraction of stroke patients can benefit from this treatment. However, even for some patients who receive the tPA treatments, reperfusions after tPA administrations have been shown to exacerbate injuries initially caused by ischemia[63]. Currently, Stent-Retriever thrombectomy was applied after tPA treatments to

increases reperfusion rates in some cases, but the long-term functional outcome improvement of this procedure is still uncertain[64]. As a result, most stroke patients suffer from long-term disabilities after stroke[9-11]; therefore it is necessary to develop new therapeutic methods that aid in long-term recovery of stroke[1].

2.1.1.1 Stem Cell Therapy

One of the main treatment options under preclinical study for stroke recovery is stem cell therapy. Stem cells are undifferentiated cells that retain self-renewal capabilities and can turn into specific cells as the body needs them[1, 65]. Embryonic stem cells and adult stem cells are two broad types of stem cells. Because of the ethical issue of embryonic stem cells, adult stem cells are frequently used in various medical therapies[66]. This treatment option aims to substitute damaged cells at the area of infarcted tissue that cannot be repaired simultaneously and assist the impaired cells which are able to potentially recover through nutrient support[1, 67]. Stem cell treatment has the potential ability to aid reestablishment of neural circuits and rebuild proper nerve conduction by replacement of glial cells[1].There are two methods for adult stem cell treatments in stroke study: the exogenous or endogenous approach[68].

2.1.1.2 Exogenous Approach of Adult Stem Cell Therapy

Exogenous stem cell method involves the transplantation of stem cells from the external to the internal. The stem cells are multiplied in culture and then transferred to the internal environment by local or systemic administration[1]. Significant recovery of function was found in rats treated with human bone marrow stromal cells at 14 days compared to control rats with ischemia. Chopp *et al*. transplanted human MSC to the stroke-induced rats through intravenous injection to test the effect of neurological functional recovery. The results shown that significant functional recovery was found in hMSC treated group compared to the control group. Also, the

amount of apoptotic cells was decreased significantly in the ischemic boundary zone in the treated group[18]. Zhao *et al.* reported that human bone marrow stem cells exhibit neural phenotypes and ameliorate neurological deficits after being grafted into the ischemic brain of rats. Transplanted human marrow stem cells survived and expressed markers of neuroectodermal cells in the rodent brain and ischemic rats showed improved neurological function after transplantation[69]. The short-term and long-term follow-up study of the application of autologous mesenchymal stem cells (MSCs) was investigated by Lee *et al.* Their results showed that the application of *ex vivo* culture-expanded MSCs is safe based on 5 years of follow-up and the mortality rate in the MSC group was lower than that in the control group[70]. This has been recognized as a promising neuroregenerative strategy to augment recovery in stroke patients[71]. However, the major restriction of exogenous stem cell therapy is the decay of the differentiation capacity of stem cells during the *in vitro* culture time, which impairs their competitiveness to be commercial grafts[72, 73].

2.1.1.3 Endogenous Approach of Adult Stem Cell Therapy

Endogenous stem cell therapy is based on the mechanism that endogenous stem cells/progenitor cells resident in organ and tissues play critical roles for organogenesis during development and for tissue homeostasis in adulthood. Even without any therapeutic intervention, the human body has a robust self-healing capability to repair damaged tissue or organs[74-79]. It has been confirmed by animal models that neurogenesis will be promoted once brain disease is present due to the fact that neural stem cells (NSC), located in the subventricular zone (SVZ), migrate to the injured area of the brain and then differentiate into nerve cells to replace those damaged cells [80-84].

Growth factors often promote cell differentiation and maturation, the effects of which varies between growth factors. Therefore, the efficacy of growth factors to promote neurogenesis of SVZ has also been tested[85-87]. For example, it has been shown that vascular endothelial growth factor (VEGF) performed an acute neuroprotective effect in the ischemic brain and promoted the survival rate of new neurons and angiogenesis. Many different growth factors are currently under investigation, such as epidermal growth factor (EGF) [88], stem cell factor[89], fibroblast growth facor-2 (FGF-2) [89-91], VEGF [92, 93], erythropoietin (EPO) [94], and BDNF [95, 96].

In the animal model, VEGF was reported to be a chemoattractant for immature neural progenitors[97]. In the study, 90 minutes Middle cerebral artery occlusion (MCAo) procedure were performed on rats to produced focal cerebral ischemia. Rats were treated with VEGF through intracerebroventricular administration had a neurological scoring grade that was improved in two motor tests and one sensory test compared to a non-treatment group and about one third of the infarct volume in each sample was reduced in the VEGF-treated group of rats[86]. The combination of EGF and FGF-2 have demonstrated that intraventricular fusion of growth factors can recruit endogenous progenitors *in situ* and hence inducing significant regeneration of pyramidal neurons after ischemia[98]. EPO treatment has also been demonstrated to significantly improve functional recovery and increase the density of cerebral microvessels at the stroke boundary[99]. The long-term anterograde delivery of high doses of BDNF is also able to potentiate the stroke-induced neurogenic response at early stages[95]. Although various successful drug delivery systems have been produced using conventional biopolymers, the lack of a system to provide successful neural regeneration demands continued investigation to identify a novel

biomaterial that can be used as delivery vehicles for therapeutic molecules such as growth factors with effective performance.

2.1.2 Decompressive Craniectomy

Even though there is a limited number of therapeutic treatments for stroke patients, there are still some choices for treating the symptoms and preventing further damage. Brain swelling is an urgent clinical problem that frequently accompanies both types of stroke[36]. DC is a standard surgical procedure performed in stroke patients to manage brain swelling. A portion of the skull is removed to relieve intracranial pressure[100-102]. The use of DC is the last choice to the surgeons since it is an invasive procedure to the patient but it can reduce mortality rate significantly[102-106]. However, it should be mentioned that the DC itself does not enhance any functional or neurological recovery outcome[101, 107].

2.1.3 Bridging the Blood-Brain Barrier (BBB)

The blood brain barrier is a protective screen of the central nervous system (CNS), which is formed by the endothelial cells of the capillary wall, astrocyte and pericytes. [108]. At the interface between the brain and blood, endothelial cells are linked together by several tight junctions, such as biochemical dimers, occluding, and claudins [109]. Overcoming the dilemma of delivering therapeutic agents to specific regions of the brain presents a major challenge to treatment of most brain diseases. Almost 100% of large-molecule neurotherapeutics and more than 98% of all small-molecule drugs are excluded from the brain by the BBB[110]. Brain drug discovery must consider improved therapeutic designs or the elaboration of efficient delivery systems. Usually, most medicines used for central nervous system (CNS) treatments are administrated via the blood circulation and for the effective drug amount to reach the target site since it is unavoidable to increase the drug dose or to prolong the period of administration time,

which is often accompanied by increasing the risk of toxicity. Only a limited number of molecules can bypass the BBB and reach the brain area in sufficient concentrations by intravenous or oral administration[111, 112]. To deliver enough amounts of therapeutics agents to the brain, it is often necessary to strategically weaken the BBB or administer drugs directly into the brain tissue in an intrusive manner, such as the application of ultrasound to open the BBB in order to allow more therapeutic drug into the brain. In addition, several studies has shown the addition or modification with PEG also is able to improve in vivo delivery to the brain through the conjugation of cell surface ligand[113, 114].

2.2 Animal Model of Stroke Study

The choice of the experiment model species and models is a key factor of success in stroke studies. This selection must be comprehensive and cautious because it is the most important aspect of experiment design. A thoughtless model may lead to unreliable data and therefore the results from animal cannot be trusted.

The use of animal models in recent decades has provided a better comprehension of the pathophysiologic mechanism of stroke. Several animal species have been applied to study stroke. The two most common species are mice and rats [115]. In addition, the cerebral vasculature and physiology of rats are similar to humans. Table 1 summaries the major rodent model of stroke research.

Table 1. Summary of rodent model in stroke

Name of Model	Advantages	Disadvantage	Reference
Intraluminal suture middle cerebral artery occlusion model	• Simulates the symptoms of human stroke	• Hyperthermia and hypothermia	[116-120]

	• Exhibition of a penumbra • Easy to control reperfusion • No need for craniectomy • Recanalization can be timed precisely • Suitable for both permanent and transient MCAo	• High risk of hemorrhage with inappropriate suture types • Not available for thrombolysis studies • Requires experienced neck surgery	
Craniotomy Model	• Higher rates of long-term survival • Successful MCAo can be determined by visualization	• Severe invasiveness and following complications • Requires an elaborate surgery	[121-123]
Photothrombosis model	• Ischemic lesion can well-defined localization • Low invasiveness • Highly reproducible	• Emergence of vasogenic edema is an abnormal feature from human stroke	[124-128]

	• Allows to study particular cell populations across animals • Ability to induce multiple silent strokes in specific area	• Study of neuroprotective agents is not suitable on this model • Little ischemic penumbra or region of local collateral flow and reperfusion	
Endothelin-1 model (ET-1)	• Low invasiveness • Low mortality • Ischemic lesion can be induced in cortical or subcortical regions • The procedure can be performed quickly • Gradual reperfusion rates are closer mimic the reperfusion in human	• Time of ischemia is not controllable • Infarcts are hard to reproduce • Interpretation of results will be complicated due to induction of astrocytosis and axonal sprouting • Need for a craniotomy	[129-131]

Embolic stroke model	• The pathogenesis is most close to human stroke • Available for study of thrombolytic agents	• Variability of lesion volume is high • Recanalization is spontaneous • Limited outcome in neuroprotection research	[132-135]

2.2.1 Intraluminal suture MCAo

In human ischemic stroke, the participation of MCA and its branches involves 70% of total ischemic stroke cases [116]. Hence, procedures that occlude this artery are the closest imitation to human ischemic stroke[117-119]. Among 2600 experiments of ischemic stroke studies, around 40% of them chose intra-arterial suture occlusion of the MCA as their stroke model[120].

The MCAo model itself does not require craniectomy and therefore it is less invasive because there is no damage to cranial structures. It has been reported that the rate of properly inducing an infarction ranges from 88% to 100% [136] that leads to about 12%subarachnoid hemorrhage (SAH)[137]. Depending on the duration of the MCAo, the striatum, the frontoparietal, the temporal cortices, some parts of the occipital cortex, the thalamus and the hypothalamus have been documented to have infarctions[138]. In mice, the areas damaged include most of the hemispheres (including most of the subventricular zone, cortex, thalamus, hippocampus, striatum) and is similar to that of rats that are subjected to MCAo[139, 140]. The scale of ischemic injury is extremely sensitive to prolonged occlusion duration in mice, as a five-fold increase in damaged volume (56±6 mm^3) is observed in the 30-minute occlusion group compared to the 15-minute occlusion group (9±2 mm^3) and also includes regions outside the MCAo region[140].

Several factors will affect the reproducibility of infarction, such as suture diameter[141], the insertion length of the suture, age of the animal, rat strain, and suture tip[142]. Silicone[143] or poly-L-lysine[144] coated sutures attach more tightly to the proximal vascular endothelium than uncoated sutures and therefore create larger infarcts and lessen inter-animal variability compared to uncoated sutures[144]. Moreover, the relation between infarct size and silicone-coating length are very strong. It is required that a length of 2.0-3.3mm should be applied to occlude the MCA in rats and longer lengths (>3.3mm) result in extended occlusion of the anterior choroidal, posterior cerebral and hypothalamic arteries.

The advantages of the MCAo model are apparent: (1) human ischemic stroke is often generated from an MCAo and therefore the model mimics pathogenesis and exhibits a similar penumbra of human stroke; (2) The MCAo model can establish a large infarct volume and have considerable reproducibility; and (3) The procedure of MCAo is relatively easy to perform. In addition, The MCAo model can also control the time of recanalization precisely and avoid opening the skull which can potential surgical injury to the brain.[120].

2.2.2 Photothrombosis Model

By utilizing the mechanism of intravascular photo-oxidation, the photothrombotic stroke model can control the ischemic lesions in the cortex[124] and alterations in striatum[125]. Intraperitoneally (mice) [125] or intravenously (rat) [124], the photoactive dye (e.g. erythrosine B, Rose Bengal) is injected and then the intact skull is irradiated by a specific wavelength light beam (560 nm) within a designed time length (20 mins). Within the irradiated area, the generation of oxygen radicals results in endothelial damage, platelet activation, and clustering in both pial and intraparenchymal vessels[145]. The target region of irradiation can be located by stereotactic coordinates to induce cerebral ischemia. The photothrombotic model is featured with advantages

of decreased rate of mortality, absence of significant surgical intervention, and high reproducibility. Disadvantages of this model is that the vessel wall was affected due to photothrombotic infarcts and the penumbra is missing in this model[126]. Furthermore, in human stroke, cytotoxic edema is a feature of acute cerebral ischemia and therefore these pathomechanisms are different compared to Photothrombosis-induced stroke. In conclusion, even though there are limitations to the photothrombotic model, it still helps to gain a visualized grasp of neuronal repair and is able to clarify the process in the perilesional area and the contralateral cortex.

2.2.3 Endothelin-1 (ET-1) model

The ET-1 model of stroke uses the potent vasoconstrictive effects that the ET-1 peptide causes[129]. This peptide can be used administered via intracerebral injection[146], application on the cortical surface[131] or directly onto an exposed MCA[147], and is able to lead a ischemic lesion with amounts of ischemic edema that is dependent on the dosage of the ET-1 injected[131, 146]. The intracerebral injection and exposed MCA method of ET-1 leaves ischemic effects similar to that of a permanent MCAo[130], while the cortical method of the peptide leaves a semicircular infarct through all the cortical layers[131]. Immediately following the use of ET-1, cerebral blood flow(CBF) is reduced rapidly and precedes several hours of reperfusion[148]. The ET-1 model is less invasive and therefore has lower mortality rates than other models. Another advantage of the model is that focal ischemia can be directly induced in deeper and more superficial areas of the brain. However, ET-1 receptors and ET-1 converting enzyme are present in astrocytes and neurons[149]. Thus, the peptide can cause astrocytosis and axonal sprouting[150] which can cause differing interpretation of results[151].

2.2.4 Embolic Stroke Model

There are two types of embolic stroke models: the microsphere-/microsphere-induced stroke model and the thromboembolic clot model. In the first model, small spheres made up of various materials like ceramic, superparamagnetic iron oxide, TiO_2, and dextran with diameters of 20-50 μm are injected into the cerebral artery with a microcatheter[132]. These spheres are then pushed through the vasculature in the brain naturally with blood flow. This microsphere model causes multifocal, heterogeneous lesions with varying severities depending on the size and dose of the microspheres[132]. Also, the related microsphere model uses bigger spheres with diameters around 100~400 μm and will induce similar results compared to the suture MCAo model with a difference in the blood supply to the hypothalamus which is conserved in the microsphere/microsphere model and thus prevents damage to the hypothalamus and prevents hypothermia[152]. One thromboembolic clot model is achieved by administering thrombin directly into the desired artery such as the internal carotid artery (ICA)[153] or MCA which induces the formation of clots[154, 155]. This model is useful because it replicates more similarly the mechanism of vascular occlusion that is common in human stroke and hence it can be used in thrombolytic agents along with[156] or in addition to neuroprotective drugs[157]. The size and location of the clot relies upon the size and elasticity of the clot that was formed[158]. Nevertheless, damage in this manner is more variable in size than a suture MCAo model[159]. In addition, some studies with thromboembolic clot models have often produced multifocal infarcts with lots of variability in the lesion size and region and even have shown an increased mortality rate, uncontrollable reperfusion and risk of cerebral hemorrhage[134, 155, 160]. It is still necessary to further improve the clot model so that they may provide the chance to investigate more exactly the pathological mechanism in animal models.

2.3 Cellulose

From the application point of view, many natural or naturally derived polymers, such as fibrin, collagen, chitosan, hyaluronan-methylcellulose (HAMC) blend, hyaluronic acid, alginate, and agarose have been studied to deliver molecules to the CNS[57, 58, 161-171]. Biomaterials may provide a useful medium through which therapeutics can be delivered directly into the brain, as some of them have a 3D network of hydrophilic polymers that can absorb significant amounts of water. Also, they can allow diffusion of the biomolecules out of the system while maintaining a physical structure and match mechanical properties of nervous tissues. Ideally, the production process of biomaterials should be easy and reliable while the sterilization of the biomaterials should happen without affecting their structural properties[51, 57, 58, 172].

In recent decades, one of the promising biomaterials is BC. Compared to the traditional plant-sourced cellulose, the BC can provide one hundred times smaller fibril which allows the related biomaterial to be more porous and absorbent. [42, 173, 174]. In addition, some research has been done to reduce the cost of mass production of BC by using environmentally-friendly methods[174].

BC can be produced by many types of bacterial strains, such as *Achromobacter* sp., *Aerobacter* sp., *Agrobactterium* sp., *Enterobacter* sp., *Psuedemona* sp., *Rhizobium* sp., *Sarcina* sp., Gluconacetobacter xylinus., Alcaligenes sp., Salmonella sp. and the *gram-positive bacterium Gluconacetobacter hansenii* , all of which have been shown to produce BC in certain culture conditions[175-177]. After BC synthesis, the harvested membrane is further processed to remove bacterial cells, organic acids and other components of the culture medium. The removal portion can be performed with several different methods, such as filtration, centrifugation, or washing.

The general method is washing the BC with a warm and diluted sodium hydroxide solution and then rinsing it with distilled water[178-181].

2.3.1 Properties

BC is a biocompatible material with a highly crystalline and pure structure[37, 38, 173, 182]. It also contains variable pore sizes so that it can hold a high capacity of water and retain its high tensile strength while fully saturated with water[27, 41, 42, 183, 184]. Its biocompatibility has been attributed to its structural similarities to the extracellular matrix (ECM)[27, 38, 41, 42, 184-186]. The BC can be modified chemically and physically by different approaches[45, 186]. For instance, the morphology of the membrane can be adjusted by the choice of containers and the production methods, the culture duration can control the thickness of the membrane, and the quality of the fibers also can be changed under the variability of media contents[42, 187-189].

The difference between the liquid versus air interactions with cellulose as it is produced causes the top and bottom surfaces of BC membranes to be different. The density will be higher on top of the BC, which corresponds to the side in contact with air, than the bottom of the BC which is more gelatinous and porous[173, 178, 190-192]. Hence, the uniformity of unmodified BC has not met the requirement to be a drug-delivering vehicle, and hence it is necessary to apply some physical or other modifications to form a homogenous membrane.

2.3.2 Tissue Engineering Application of BC

In recent years, the application of BC for TE has attracted a significant amount of attention[193]. Several studies have been determined the biocompatibility and feasibility of BC. Human vein endothelial cells (HUVEC) have been shown to grow and migrate into the inner part of the BC hydrogels structure[187]. Moreover, it also determined that a consistent layer of osteoblast was formed on the BC after human adipose-derived mesenchymal stem cells (HASCs)

were cultured on the BC substrate. In addition, BC material were used ulna defects of rabbits, the obvious mineralization was detected in the injury site without any inflammation symptoms when compare with control group after 8 weeks[194].

To teste the biocompatibility of the BC in *in vivo*, the BC was subcutaneously implanted on the back of Wistar rats. Foreign body reactions, chronic inflammation, angiogenesis, and cell growth were investigated after three months. The results of this study showed that BC was completely able to become a part of the host tissue and no evidence of inflammatory reactions were observed during the experimental period[195]. The BC synthesized by Kombucha was also fabricated into a tube shape and cultured with primary Schwann cells before being transplanted into Sprague Dawley rats with nerve injury over six weeks. The BC tubes showed excellent biocompatibility [196]. Also, the BC tubes were tested as a replacement small-diameter blood vessel. Schemer *et al.* implanted the tubular hydrogels from bio-designed cellulose to replace the carotid arteries of sheep *in vivo* and observed formation of immigrated vascular smooth muscle cells along the BC scaffold without signs of prothrombogenic or inflammatory potential.[197]. Table 2 has shown the summary of BC applications in TE.

Table 2. Summary of BC applications in TE

Application	Experiment	Results	References
Wound dressing	Evaluation of skin regeneration and angiogenesis in burn injury skin of Sprague-Dawley rats by BC membrane	Bacteria cellulose membranes (BCM) may accelerate the process of wound healing in burn injury skin of rats through regulation of angiogenesis and connective tissue formation	[198]

	BC pellicles were immersed in a zinc acetate solution and then crystallized	The antibacterial activity of the nanocrystalline ZnO particle-incorporated BC sheet against gram-negative and gram-positive bacteria is strong	[199]
	Microbial cellulose formed/coated on cotton gauze samples during its biosynthesis in a static medium for 6 days by Acetobater Xylinium	Cotton gauze coated with microbial cellulose increases water absorbency and wicking ability over 30%, and reduces drying time by about 33% that can be concluded to promote some important characteristics for wound dressing	[200]
	A freeze-dried BC film was immersed in a benzalkonium chloride solution, followed by another freeze-drying step	Stable and prolonged antimicrobial activity for at least 24h was obtained especially against some bacteria that were found on the contaminated wound	[201]
	Sliver nanoparticles with an average diameter of 1.5 nm were well dispersed on bacterial cellulose	Ag nanoparticles are well dispersed on BCF surface via chemical-reduction and presents excellent antibacterial property	[173]

	nanofiber (BCF) via a in situ chemical-reduction	and can be used as a functional antimicrobial agent	
	Antimicrobial bacterial cellulose-sliver nanoparticles composite membranes were fabricated from hydrolytic decomposition of sliver nitrate solution using triethanolamine as a reducing and complexing agent	The composite membranes exhibited strong antimicrobial activity against Gram-negative and Gram-positive bacteria	[202]
	An aloe-cellulose composite membrane was developed by amounts of adding aloe vera gel in the culture medium during static cultivation	A fibre-reinforced bio-polymer film displayed significantly improved properties in mechanical strength, water absorption capacity and water vapor permeability and is expected to have a wide range of application	[203]
Cardiovascular implants	An anisotropic Polyvinyl alcohol (PVA)-BC nanocomposite was	PVA-BC nanocomposites with a controlled degree of anisotropy that closely matches the	[204]

	prepared by using a novel processing method under an applied strain and with the addition of some BC nanofiber	mechanical properties of the soft tissue ranging from cardiovascular to other connective tissues	
	The tubularly shaped bacterial synthesized cellulose was designed during the cultivation with the aim to develop biomaterial for medical application	Great water retention values, low roughness of the inner surface, excellent mechanical strength in wet state demonstrate the high potential as an artificial blood vessel in microsurgery	[178]
	A novel BC-chitosan/heparin composite was prepared and tested on the MC3T3-E1 cells	The 3-(4,5-dimethylthiazol-2-yl)-2,5-diphenyltetrazolium bromide results indicated that the BC–chitosan/heparin composites were suitable for cell proliferation and ingrowth.	[205]
Cartilage scaffolds	Native and chemically modified BC materials secreted by Gluconacetobacter xylinus	Unmodified BC showed significantly higher levels of chondrocyte growth and modified BC performed to mimic the	[206]

	were evaluated using bovine chondrocytes	glucosaminoglycans of native cartilage	
	Porous bacterial nanocellulose (BNC) produced by gluconacetobacter xylinus was investigated with human primary chondrocytes derived from routine septorhino- and otoplasties	Human primary chondrocytes were able to adhere to bacterial nanocellulose and produce cartilaginous matrix protein such as aggrecan (after 14 days) and collagen type II (after 21 days) in the presence of differentiation medium	[207]
	BNC is investigated for use in ear cartilage TE and the mechanical properties of native ear cartilage are measured for preliminary benchmark for ear cartilage replacement material	BNC can be fabricated into patient-specific auricular shapes and has the capability to reach mechanical properties of relevance for ear cartilage replacement	[208]
	The mechanical properties of BC gel were compared with a collagen material and the meniscus	The Young's modulus of bacterial cellulose and meniscus are similar in magnitude under a compression load of 2kPa and with five times better mechanical	[209]

		properties than the collagen material	
Bone scaffolds	Bacterial cellulose-hydroxyapatite (BC-HA) nanocomposite membranes were evaluated in noncritical bone defects in rat tibiae at 1,4, and 16 weeks	*In vivo* tests showed no inflammatory reaction after 1 week and defects were observed to be filled in by new bone tissue and hence the BC-HA were effective for bone regeneration	[210]
	BC scaffold cultured by A.xylinum X-2 and were investigated for osteogenic potential with BMP-2	BC had a good biocompatibility and induced differentiation of mouse fibroblast-like C2C12 cells into osteoblasts in the presence of BMP-2 *in vitro*	[211]
	BC scaffolds were cultured with paraffin wax microspheres and then were removed before seeding with MC3T3-E1 osteoprogenitor cells	Cell clustered within the pores of microporous BC and formed denser mineral deposits than cells grown on control BC surfaces confirmed that it is a promising biomaterial for bone TE applications	[212]
	BC incorporated with high dose antibiotics were	The properties of compression strength, fracture toughness, and	[213]

	compared to traditional antibiotic cement under compression strength, fracture toughness, fatigue life and elution kinetics test	fatigue life of the cellulose antibiotic cement are all better compared to traditional antibiotic cement and cumulative elution over 35 days	
	A multicomponent organic/inorganic composite BC-gel/hydroxyapatite double-network (HAP-DN) was synthesized in order to improve the mechanical strength of BC/HAP	The innovated BC material has been shown to have rougher surface topography, higher thermal stability and *in vitro* cell culture demonstrated that it had better adhesion and higher proliferation ability	[214]
Dental Treatments	BC was evaluated for its applicability as a novel material for dental canal treatment regarding solution absorption, expansion, tensile strength, drug release and biocompatibility	BC has excellent material and biological characteristics compared with conventional material and higher absorption and expansion than a paper	[215]
	Synthesis of a composite polymer with 3D structure	The hydrocompounds exhibited an increased structuring degree	[216]

	consisting of biocellulose and minerals binder power through sol-gel technique	and favorably adhered to the surface of the embedded biocellulose particles	

2.3.3 BC used for Drug Delivery Applications

Although BC has been used in many fields of TE, it has also shown considerable potentials to be a drug delivery system. The BC, before drug loading, can be sterilized by heat and Ultraviolet treatments which are both effective, fast, simple, and without any toxic residue sterilization techniques[51]. Therefore, BC has been used as a releasing platform by several methods. For example, After loading berberine into BC, it can extend release by 80% for 20 hours compared to commercial tablets, which release almost all of a drug in the first hour after oral administration[217, 218].

BC has also been tried to be combined with GF as well. Shi *et al* explored the possibility of BC loaded with BMP-2 to be utilized as a localized delivery system to increase the local concentrations of cytokines for TE. Their results showed that BC had good biocompatibility and induced differentiation of mouse fibroblast-like C2C12 cells into osteoblast in the presence of BMP-2 *in vitro*, and the *in vivo* subcutaneous implantation studies showed that the BC loaded BMP-2 group had more bone formation and higher calcium concentration than the BC alone group. This study suggests that BC can be a great localized delivery system for GF and a potential candidate in TE[211]. In other words, it also shown that the BC has potential to be a novel duraplasty which can release therapeutic molecules to promote the brain recovery after stroke.

2.4 Functional Assessments in the Rodent Stroke Model

Functional impairments are common after stroke; functional outcome in animal models has offered a better perspective to the biological foundation and potential recovery efforts of experimental stroke. Establishing and utilizing tests that can recognize behavioral disorders is basic to exploring the progression of therapies. Meanwhile, there are no flawless functional assessments of animal models since different tests are sensitive to different areas of impairment, from local to global, after stroke as shown in Table 3. It is essential to consider the selection of tests based on both the area of the brain injury and the applied treatment. Most behavioral tests concentrate on motor and sensory monitoring because of the reduction of limb function after stroke. Impairments in memory and studying are also usual after stroke and therefore cognitive function tests are also a key component in analyzing the overall scope of deficits. Several issues may arise and be considered during choosing and conducting functional evaluations, which include ethical questions and time feasibility of task training. Furthermore, since spontaneous recovery normally happens in animals, designing a good timeline to perform testing after surgery must be taken into consideration cautiously as well.

Table 3. Summary of functional assessments

Name of test	Symptoms evaluated	Advantages	Disadvantages	References
Adhesive removal test	Sensory function	• High sensitivity for MCAo model with small cortical damage	• Pretraining needed • Minor response rate in models without cortical injury	[219, 220]
Staircase test	Fine motor coordination	• Can be used for long-term study • Results are reliability	• Several animals are excluded • Long-time pre-training required	[221, 222]

Beam walking test	Motor coordination	• Excellent sensitivity in both rats and mice after ischemia	• Pre-training needed • Reparatory deviation without a ledge	[223, 224]
Corner test	Function of Whiskers	• Easy and quick • No-training needed • Assesses long-term dysfunctions in striatal damage	• Limited efficiency if lesion in the cortical area only • Low demonstration in rats' model	[225, 226]
Rotarod test	Motor balance	• Great reliability in rats • Replicable from lab to lab	• Worse sensitivity in mice model after three days of MCAo	[227, 228]
Open field test	Locomotor activity	• Able to assess emotion • No animal handling during testing	• Only works for short-term observation • Poor performance with minor infarcts	[229, 230]
Elevated body swing test	Muscle strength	• Simple and fast • No training needed • Sensitive even one month after MCAo	• Not common in ischemia model	[231, 232]
Cylinder test	Motor coordination	• Easy to perform • Nice sensitivity with/without striatal damage	• Poor sensitivity with small infarcts	[233, 234]
Food-fault test	Motor coordination	• Proper test for neuroprotection studies	• Can only be used on animal with severe stroke	[235, 236]
Morris water maze	Memory and learning ability of spatial	• Durable sensitivity in rats for long-time observation after ischemia	• Less sensitivity in mice model after three days of MCAo • Pre-training required	[237, 238]

Passive avoidance test	Avoidance learning	• Easy to perform • Great performance on both long-time study of rats and mouse after ischemia	• Equipment may be expensive • Pre-training needed	[239, 240]
Neurological scales	Balance, muscle strength, motor coordination and reflexes	• Provides a comprehensive view of the ischemic damage • Simple and quick	• Poor sensitivity in long-time observation • The score is subjective by manipulator (double blind)	[241, 242]

2.4.1 Bederson Scale and Neurological Scoring Scales

The Bederson Scale is a universal neurological assessment that was invented to measure neurological impairments following exhibition of various deficits after stroke[243]. Forelimb flexion, resistance to lateral push and circling behavior are evaluated in the test. The grading scale is from 0 to 3 to assess behavioral deficits after stroke and it is an easy method to detect neurological deficits. Animals with ischemic stroke will have a significantly higher score compared to non-surgery animals because of the amounts of neurological deficits after stroke[244-246]. Several updated scales have been designed by improving and modifying the simple methods to detect impairments based on the Bederson scale[246-248]. Even though this evaluation is simple to complete, the subjectivity of it limits the neurological rating of the scale. Moreover, it cannot be used in the detection of long-term deficits after stroke due to that fact that some functional deficits will no longer be detected based on the Bederson scale method over the time.

2.4.1 Modified Neurological Severity Scores (mNSS)

Modified Neurological Severity Scores (mNSS) is one of the most widespread neurological scales used in studying strokes in animal studies. The scale of mNSS to rate neurological functioning is 14 for mice and 18 for rat, respectively. It consists of balance , reflex, muscle status, abnormal movement, visual, tactile and proprioceptive tests[244, 249]. The neurological rating score gives the opportunity to evaluate multiple deficits and can be performed very well for a long-term period of 30-60 days although spontaneous recovery can be observed during this time[225].

2.4.2 Cylinder Test

Expeditionary behavior in the animal models offers a chance to investigate the neural basis of functional behavior which can be applied to the analysis of brain function[250]. The cylinder test is also known as the limb-use asymmetry test and it was first presented by Schallert *et al.*[251]. It provides a method to assess the rodent's spontaneous forelimb use and has been extensively used animal stroke studies after motor functional damages[227, 251-254]. In order to assess forelimb deficits, the animal is placed in a lucid plastic cylinder and inspected. The animal will automatically communicate with vertical surfaces by raising their hindlimbs and using their forelimbs and vibrissae to touch the surface. During the monitoring of cylinder tests, the times of independent wall placement for both forelimbs, right forelimb and left forelimb are counted. Animals that have unilateral brain injury will exhibit asymmetry in forelimb use during interaction with the vertical wall[255]. The cylinder test is a simple, objective, sensitive method to detect chronic deficits that avoid personal factors and it also can been used in those animals which only have mild neurological defects[254, 255]. Even though the cylinder test doesn't require pre-training, it is better to receive baseline data for bias correction due to the fact that some animals show a preference of independent use of a single limb[251]. In addition, it has been reported that

performing the test under the dark cycle of the animal and red lighting conditions gives the best results because rodents are more prone to searching in a dim environment[254].

2.4.3 Staircase Test

Montoya *et al.* first exploited the staircase test to observe the use of forelimbs after unilateral or bilateral cortical damage[221]. It was primarily designed for rat models and then adapted to mice to quantify the animals' ability to grab food pellets which are set up in grooves of the staircase. Animals have to be pre-trained for 15 days prior to the test under food-deprivation conditions with the aim to achieve a reduction of 10% of their original weight. Those rats that are unable to pass the training session are removed from the study. This intricate task evaluates both subtle motor coordination ability and missing sensory function[221]. It displays an excellent sensitivity with convincible results from long-term studies after MCAo stroke[256-259]. Research has shown a correlation between sensorimotor deficits and the lesion volume by the staircase tests[256, 258, 259]. Despite self-recovery during the first 14 days after the damage was reported in several studies[256, 257], the staircase can even be used two months after stroke with fine sensitivity[258]. One advantage of this test is that it can either evaluate cortical damage[259] or tiny striatal lesions[257]. Up to now, considering the long training time required and the fact that some animals may be excluded before the test, the staircase test is not commonly used in animal stroke model evaluation. However, it is still a scientific and exact test for the assessment of long-term functional recovery in neuroscience studies.

2.4.4 Beam Walking Test

The walking beam test is an alternative method to evaluate motor coordination. It is originally described by Feeney *et al.* [223]. It aims to assess the animal's ability to cross a narrow beam to reach an enclosed platform. The beams are made of wood strips and can be square (1m length with

28mm,12mm, or 5mm cross sections) or round (28mm,17mm, or 11mm diameters)[260]. Subsequently, a step-down ledge was introduced to the beam in order to avoid full slippage of the limb[261]. The installation of the ledge blocks the animals from compensatory strategies, which may affect the final result[262]. Baseline data is also required before ischemic surgery so that it can be compared with post-surgery trials. This test has been extensively adopted in both permanent and transient focal cerebral ischemia rodents' models and produced trustworthy data and significant differences between surgical groups and sham groups even after 20-30 days of MCAo. The relationship between infarct size and performance of neuronal migration and neurogenesis are also presented by this test[263]. It is important that the test is able to determine and distinguish the effects influenced by neural repair rather than the learning of compensatory strategies in chronic studies which make it an effective test for stroke studies focused on neuro-repair.

2.4.5 Adhesive Removal Test

The adhesive removal test, also known as the tape removal test, was first presented by *Schallert et al.*[253]. It evaluates the ability of a rat to touch and remove an irritation from its forepaws and is further optimized for mice[219]. During this test, two pieces of tape with defined sizes are placed on a part of each paw where they are not covered by hair with the same pressure. After that, the animal is placed in a lucid box and two timepoints are recorded: (1) time to contact, it is the time that the animal starts to feel the labels and takes them in its mouth; (2) time to tape removal, it is the time from contact until the tape is removed. For this evaluation, it is better to obtain baseline data by pre-training for recognizing any preoperative asymmetries and better performance in the post-surgery test[245, 254]. It is also necessary to keep consistency within the testing environment such as consistency in home cage, because tiny factors can influence the functional outcome[254]. The adhesive removal test is one of the most common sensory tests used

in rodents especially in rats of MCAo model for both short- and long-term studies[248]. It can identify functional impairment correlated with the lesion size up to 26 days[225] and 11 weeks[250] after ischemic stroke. In addition, sensory neglect caused by distal MCAo which induces small cortical lesions is also able to be detected[252]. However, it is also noted that the sensitivity of this test may be impaired when a short-term intraluminal MCAo doesn't induce a cortical lesion[249]. Even though the adhesive removal test still has some aspects that need to be improved, it is still a reliable, sensitive and useful protocol to assess functional outcomes for neuro-repair and neuroprotection research after MCAo.

2.4.6 Ladder Rung Walking Test

In order to determine even subtle loss of movement capacity, the Ladder Rung walk was originally developed for rats[264] and then optimized for mice later[265]. The measurement of placing, stepping, and the coordination of inter-limbs are the main purposes of this test[264]. The device consists of a horizontal ladder and rungs, where the distance between the rungs can be adjusted in order to avoid the offset reliance via learning of the spacing and location of the rungs[264]. Video of foot faults are analyzed to calculate a score on a rating scale based on the quality of limb placement. This method doesn't need any long-term training for chronic stroke testing and animals with motor system damage have displayed deficits in the ladder rung test after stroke[234, 264, 265].

2.5 Duraplasty

Over the years, various options for many different types of duraplasty have been manufactured. A quality duraplasty material should meet all the following criteria. The duraplasty material must be biocompatibility with no danger of infection. Moreover, it should have enough mechanical strength to be able to survive the implantation surgery, while still conserving elasticity

and flexibility so that it can mold into the shape of the brain. Furthermore, it must be sealed watertight to block CSF from leaking through the material. Duraplasty has usually come in different types of materials: autografts, allografts, xenografts and synthetic materials.

2.5.1 Autograft

The definition of an autograft is using a material that originates from the individual themselves. In some surgeries, the surgical area is limited and hence the replaced material cannot be taken from original site. The current solution involves obtaining material from other parts of the body to use it therapeutically[266-272]. In addition, no rejection problem or disease transmission from the graft materials is expected with autografts. However, patient morbidity is increased because another surgery on a different area of the body is necessary[268, 269, 271, 273]. The fibrous tissue deep in the thigh is generally used for dural replacement. Other tissues have been used as well such as the temporalis fascia, muscle, the pericardium, and fat[268, 272-275]. Autografts seem to have higher incidences of septic meningitis, CSF fistulas, and overall implant failure than other types of grafts[272, 276, 277].

2.5.2 Allograft

Material used for duraplasty that originates from a different individual from the same species as the recipient is called an allograft. Previously, cadavers provided the source of the materials, but this has led to limited availability of allografts. Additionally, this method seems to lead to increases in the transmission of prion diseases and viral infections[266, 268, 278-281]. A different source of this material could be human amniotic membrane[282]. However, like fetal stem cells, this raises many ethical concerns and is also hard to obtain due to small quantities being available[283].

2.5.3 Xenograft

When a material is sourced from a different species, which many times involves collagen being taken from animal tissue, it is a xenograft[280, 284]. Usually, using collagen in this manner causes it to have low mechanical strength due to the solubilization in acetic acid for re-shaping that results in a loss of structure compared to the original matrix[285]. This can be a problem because CSF leakage and pseudomeningocele have been observed due to the material being prone to thinning and hole formation[286, 287]. Immunological issues, including the risk of transmission of animal pathogens or infections, also exist in these materials[284, 288-291]. Treatments such as hydrochloric acid or sodium hydroxide are established to neutralize potential prions[269-271, 279, 292]. Codman Duraform® Dural Graft made by Johnson & Johnson in New Brunswick, New Jersey is a currently available commercial xenograft. Duraform® is made of type I collagen tissue harvested from a bovine Achilles tendon. A minimal inflammation reaction was observed but, because it is absorbable, this disappeared with time. The material demonstrated decent handling qualities and was able to prevent CSF leakage[293].

2.5.4 Synthetic Duraplasty

One of the greatest advantages of the synthetic duraplasty is it can be manufactured easily into various shapes and size and this makes it very useful[294]. They also offer less risk of transmitted diseases [268]. Synthetic materials that are both absorbable and non-absorbable have been used. Permanent implants are made up of non-absorbable material, whereas the body slowly absorbs absorbable materials, and therefore the latter have the benefits of not causing chronic inflammation unless degradation products elicit it[294]. There are several materials that have been made into synthetic duraplasty, such as BC[266], silk fibroin[295, 296] and polytetrafluoroethylene (PTFE)[297-299]. For example, *Shi ,et al* have used biocompatible

poly(lactic acid)(PLLA) fibers to test the safety and effectiveness of this biomimetic patch for dural repair[294]. The results show that the patch has excellent mechanical strength and tissue biocompatibility. In addition, it achieves complete degradation within a two-year period to prevent leakage which shows its potential as an artificial dural substitute. Another duraplasty named Synthecel (Depuy Synthes, Raynham Massachusetts) is composed of biosynthesized cellulose. It was first investigated by *Rosen et al.*[266]. The researchers show that it has a limited foreign body response and a similar thickness and conformation compared to human dura[300, 301]. Also, it has shown better ability to prevent CSF leakage than xenografts[266].

It is worth noticing that xenografts and synthetics duraplasty have been commercialized for a long time, however, there is no research or lab that has focused on using duraplasty as a drug-delivery platform and therefore the duraplasty doesn't have any recovery outcomes up to date. In other words, it is an innovative field that looks to combine the synthetic duraplasty and drug-delivery system for endogenous stem cell therapy.

3. Objectives

3.1 Motivation

The motivation regarding this project was to design a local target drug delivery platform which can overcome the clinical impracticality of intraventricular injection and other therapies. The design combines various fields such as biomaterials, stem cell therapies and animal pathologic model. Since the duraplasty is usually applied to cover the surface of the brain after DC but does not enhance functional and neurological outcome, the idea was to take advantage of the "open" opportunity that is offered by DC procedure by bioengineering a specialized regeneration factor-releasing duraplasty biomaterial that can be placed on the brain at the time of DC to promote recovery after stroke

In this work, we hypothesize that the duraplasty fabricated from blended biosynthesized cellulose developed by our lab, with incorporated growth factors, can be implanted during a regular DC procedure to enable bioactive molecule deliveries to the injured area after stroke for enhanced functional recovery.

3.2 Objectives

The following missions are the objectives for this thesis:

Objective 1: Optimization of duraplasty fabrication procedure and characterization of duraplasty;

Objective 2: Investigate the biocompatibility and applicability of duraplasty by in vivo animal study;

Objective 3: Establishment of a rodent stroke model which can be used to assess recovery after treatment;

Objective 4: Assessment of the distribution and penetration of growth factor in the in vivo rodent stroke model

4. Materials and Methodology

4.1 Materials

The bacterial strain (*Gluconacetobacter hansenii*) was purchased from American Type Culture Collection (ATCC©, Manassasm, VA). It was incubated in a modified Hestrin-Schramm culture media, which consisting of glucose (20.0 g/L), yeast extract (5.0 g/L), peptone (5.0 g/L), disodium phosphate (2.7 g/L), and citric acid (1.5 g/L)[302]. Initial BC membranes were harvested in a static cell culture at 26°C after 7 days. The BC membranes were purified by soaking them in 0.1M NaOH at 50°C for 24 hours under agitation in order to remove endotoxin and then rinsing

them by distilled water until PH of the solution had reached neutral pH. The membranes were kept in the refrigerator for further use.

4.2 Methodology

4.2.1 Fabrication of Blended Biosynthesized Cellulose Duraplasty

To produced BBC duraplasty, the purified BC membranes were mixed with a certain amount of distilled water in a blender for 3mins (Oster®, Brampton, ON) to produce the homogenous pulp. In order to obtain consistent BBC duraplasty, calculations were performed figure out the amount of cellulose pulp needed at the beginning of fabrication. The pulp was weighed and then filtered by using a 40C Buchner fritted disc filter (Kimble Chase, Rockwood, TN) for 40mins under 0.6 MPa of vacuum pump to form a paper-like sheet. The filtered sheet was weighted and then frozen under -20 °C for 24 hours, which was subsequently lyophilized at -80° C under vacuum (Labconco Corporation, Kansas City, MO) for 48 hours. The mass of the freeze-dried sample was weighed again and compared to that before the lyophilization. Due to the homogeneity of the cellulose pulp, there should be a positive correlation between the mass of pulp and that of the freezing-dried. All fabricated BBC were sterilized via autoclave before further use. This procedure is shown in Figure 1.

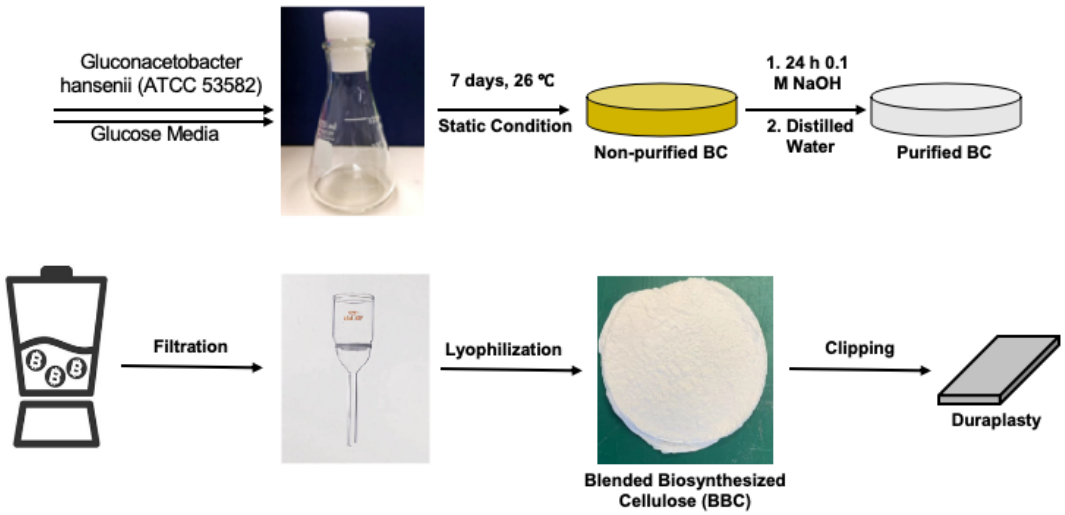

Figure 1. Schematic of BBC duraplasty fabrication

4.2.2 Mechanic Test Protocol

Tensile tests were conducted on the swollen duraplasty samples to characterize the mechanical properties of the prepared duraplasty. The measurements were carried out at 25 ± 2°C and relative humidity of 45±5% on an Instron ElectroPuls^{TM} E3000 All-Electric Dynamic Test Instrument (Instron, Norwood, MA) equipped with Instron® Bluehill® Software (Instron, Norwood, MA). Filter paper was applied between the grips of the mechanical tester and the sample, on both sides of the sample to assist prevention of slippage, and 7.5 mm of the sample were handled by the clamps on each sides of the sample. The crosshead speed was set at 5 mm/min and load cell dynamic rating of ± 250 N was applied. Load-extension curves were recorded and used to measure Young's Modulus, ultimate tensile strength and elongation-at-break.

4.2.3 Swelling Ratio Protocol

The swelling ratio (SR) of duraplasty was tested by a gravimetric method. Duraplasty 1-6 samples were immersed into 15 mL of distilled water at 25 °C for 72 hours; then the rehydrated samples were weighted in a designed time interval. The final mass of the samples is recorded as M_{wet}. The SR of the duraplasty was analyzed by the Equation 1.

$$\mathrm{SR} = \frac{(Mwet - Mdry)}{Mdry} \times 100\% \qquad (1)$$

4.2.4 Scanning Electron Microscope (SEM) Analysis

To study the morphological of the BBC duraplasty samples, a Phenom Pro scanning electron microscope (Nanoscience Instruments, Phoenix, AZ) was used. Random selected samples were stuck onto aluminum stubs through the carbon-based double-side adhesive discs with electrically conductive. Images of both sides of the duraplasty and its cross section were obtained in the microscope at an accelerating voltage of 15 kV.

4.2.5 BSA-Loading and Release Analyses

Bovine serum albumin (BSA) was used as a model protein drug and six samples were investigated as drug delivery system. The duraplasty sample in this analysis were cut into rectangular shape matching the size of removed skull in the following *in vivo* studies (3mm x 5mm). Subsequently, samples were placed in a 24-well plate and 10 μL of a solution of 7000 μg/mL (w/v) of BSA in pH 7.4 PBS solution was pipetted on the top of each samples. The samples were kept in static for 2 hours until the BSA solution was totally absorbed by the membrane and then transferred to 6-well plate. To investigate the drug delivery performance of the duraplasty, the prepared duraplasty was fully submerged in 2 mL of PBS (pH7.4) at 25°C. At each pre-determined time intervals, 0.45 mL releasing buffer was collected and supplemented with the same volume of fresh PBS. Concentrations of BSA from the collected buffer were quantified with a micro BCA protein assay kit (Thermo Fisher Scientific, Waltham, MA) following the manufacturer's instructions and the absorbance was measured at 562 nm using an Epoch™ microplate spectrophotometer (BioTeck, Winooski, VT). The amount of released BSA was determined from the standard calibration curve. The cumulative amount of BSA released was calculated by Equation 2.

$$R = (Cn * Vo) + \sum_{i=1}^{n-1} (Ci * Vi) \quad (2)$$

The cumulative amount of BSA released at each time point is presented by R, Cn is the measured concentration from the BCA assay and Vo is the total volume of the sample at that time point. The previously measured concentrations from the BCA assay were all treated as Ci, and Vi are the aliquot volumes which were removed from the sample at each time point. The initial burst was calculated using Equation 3.

$$Burst\ Release = \frac{Cumulative\ amount\ released\ after\ 24\ hours}{Total\ cumulative\ amount\ released} * 100\ \% \quad (3)$$

4.2.6 In vivo animal analyses

All animal studies were performed in strict compliance with the Guide to the Care and Use of Experimental Animals prepared by the Canadian Council of Animal Care and protocols approved by the Animal Care Committee of the Ottawa Hospital Research Institute.

4.2.6.1 *In vivo* Biocompatibility Studies

To explore the biocompatibility of the BBC membrane as a duraplasty, blank BBC duraplasty samples were implanted in rodents over the removed area as part of a DC procedure. Adult female Sprague-Dawley rats, 9-10 weeks of age (Charles River, St. Constant, QC) were injected 5 mL of saline prior to surgery and then anesthetized by inhalation of 4% isoflurane for induction and then reduce to 2% during surgery for maintenance during surgery, in combination with oxygen supply at 2L per minute. The rat was placed in a stereotaxic unit and a middle incision was made from the eyes to the base of the ears. A rectangular hole was drilled into the skull running from + 2 to -3 mm anterior/posterior to the Bregma and running laterally from -1.5 to -4.5 mm from mediolateral. The dura in the exposed hemisphere was removed and the duraplasty was placed on top of the brain. The animals were then sutured, and topical analgesic was then applied

along the surgical incision site. Buprenorphine was provided at 1mg/kg to maintain analgesia for 72 hours post-decompression. Rats were sacrificed at either 1week or 4 weeks post-DC for analysis.

4.2.6.2 Hematoxylin and Eosin Staining

At the time of euthanasia, the animal was anesthetized with inhalation of 5% isoflurane, followed by intraperitoneal injection of sodium pentobarbital. The animal was then perfused by PBS (pH 7.4) and following 4% paraformaldehyde (PFA) solution by transcardial perfusion until the whole body is rigid. The whole brain was dissected and fixed in 4% PFA for 24 hours and then tissue was dehydrated in 10%, 20%, 30% sucrose solution each for 24 hours. For the sectioning of brains, the brain tissue was embedded in optimal cutting temperature compound (OCT) (Sakura Finetek, Inc., Torrance, CA) under dry-ice cooling isobutane and sectioned coronally into 20 μm serial section and collected on Superfrose slides (Thermo Fisher Scientific, Waltham, MA). For hematoxylin staining, sections were dried for 30 minutes and washed in deionized water to remove OCT. Sections were stained with hematoxylin solution for 5minutes, washed with deionized water. Sections were then stained in Eosin Y for 5 minutes, and dehydration in increasing concentrations of ethanol (70, 80, 90, and 100% v/v) and xylene[303]. Sections were mounted on coverslips using permount (Thermo Fisher Scientific, Waltham, MA).

4.2.7 Behavioral analysis following a 60/90 minutes MCAo times in rats

In order to determine the ideal occlusion time of a stroke for further stroke study, two groups of animals were compared. The model of MCAo was used to produce the stroke and the occlusion time is 60 and 90 minutes, respectively. In total, 26 male Sprague-Dawley rats weighing approximately 300 g at the time of surgery were used in this study. Once arrival, animals were acclimatized to the housing facilities and handled daily for 4 days. Baseline performance for the Montoya Staircase, horizontal ladder, forelimb use asymmetry (cylinder), adhesive tape removal

and beam walking tests was measured from 15 days to 5 days before the surgery (Figure 2). On Days 25 to 29 (Week 4) and 52 to 56 (Week 8) after surgery, all rats were assessed on the Montoya staircase, horizontal ladder, forelimb use asymmetry (cylinder), adhesive tape removal and beam waking tests.

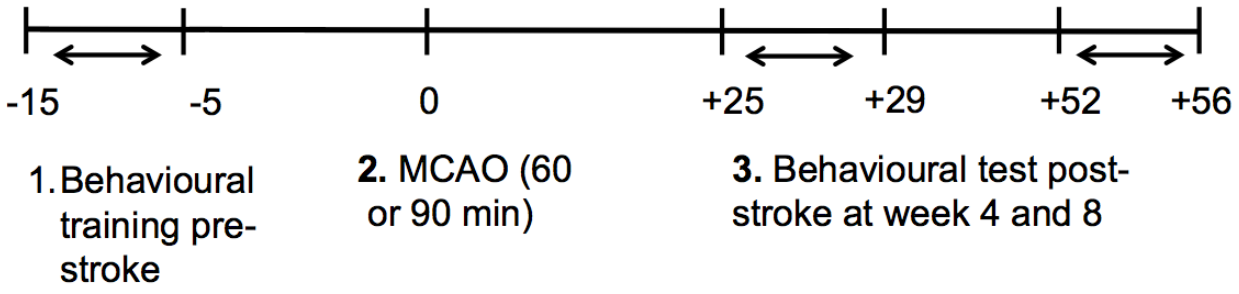

Figure 2. Timeline of Behavioral Study

4.2.7.1 Surgery of MCAo in Behavioral Assessments study

On the day of the surgery, rats were given 5 mL of saline prior to surgery. Rats were anesthetised with isoflurane (4% to induction, 2% maintenance isoflurane and oxygen). The animals were resting on a heating pad to ensure body temperatures do no drop during the surgery. Under aseptic conditions, a midline incision along the neck was made to expose the carotid artery. Ligatures was placed around the common carotid artery and the external carotid artery. Clamps were used to prevent the ligatures from loosening and to prevent bleeding. Focal ischemia of 60- or 90-minute duration was randomly assigned and induced by the filament method (4.0 surgical suture-2 cm in length, Doccol Corporation, Sharon, MA). The filament was inserted into the internal carotid artery to block the middle cerebral artery. After the suture was in place, the incision site was closed with surgical staples and the animal was carefully placed into the recovery cage with a heating pad under one side of the cage. Shortly before the end of the 60- or 90-minute occlusion period, the rat was re-anesthetized and surgical site was re-sterilized and re-opened. The

suture was removed at the end of the occlusion time. At this point reperfusion occurred, Microclips were removed and the external carotid artery ligated. The surgical incision site was sutured, and topical analgesic applied along the incision site. Animals were placed in recovery cages with a heating pad under one side of the cage again and monitored until there are awake.

4.2.7.2 Horizontal-Ladder Walking Test

Rats were videotaped crossing the middle segment of a 1 m long horizontal ladder with variable spaced rungs ranging from 3 to 5 cm. Four trials per test day where the number of hits and number of slips made with each limb was recorded. A detailed analysis of stepping was performed for baseline, day 28 and day 56. This test assessed both forelimb and hindlimb placements. The percentage of successful steps was calculated as Equation 4.

$$\%\ successful\ steps = (1 - [foot\ faults/total\ steps]) \times 100\% \quad (4)$$

4.2.7.3 Cylinder Test

Rats were placed in a transparent cylinder (20 cm diameter, 30 cm tall) for 5 minutes and videotaped from below. Wall exploration and forelimb use were analyzed. Wall exploration is the placement of the forelimb on the wall and contact during lateral movements. The number of ipsilateral and contralateral wall forelimb contacts was determined from videos. This test assessed asymmetrical limb use of animals for postural support[304]. The percentage of impaired forelimb use was calculated based on a previously published protocol[251] as shown in Equation 5. For each test period, one trial was conducted to all rats.

$$\%\ \text{use of impaired paw} = \left(\left[\text{contralateral contacts} + \tfrac{1}{2}\ bilateral\ contacts\right]/total\ contacts\right) \times 100\% \quad (5)$$

4.2.7.4 Adhesive tape removal test

Adhesive dots were placed on rat's forepaws. On three trials, the time taken to touch and

remove the adhesive dots from each paw was recorded. This test assessed sensory and fine motor skills of animals. An asymmetry score was calculated as Equation 6.[251]

$$\sum \frac{(time\ to\ remove\ dot\ contralateral\ paw - time\ to\ remove\ dot\ from\ ipsilateral\ paw)}{number\ of\ trials} \quad (6)$$

4.2.7.5 Beam Walking Test

Rats were videotaped while crossing a 160 cm long elevated/tapered, 2-level beam to reach a dark goal box containing food pellets. Training consisted to let the rat cross the beam from the beginning until the end without any pauses. The performance was determined by the average of the 4 trials per day. On the day following the training, baseline performance was assessed. Following the stroke, the performance was assessed by the number of hits or slips for each fore- and hindlimbs. This assessed both forelimb and hindlimb placements[304]. The percentage of successful steps was calculated as Equation 7. [305]

$$\%\ successful\ steps = (1 - [foot\ faults\ /total\ steps] \times\ 100\%) \quad (7)$$

4.2.7.6 Montoya Staircase Test

Rats were food deprived 4 days before testing. Rats performed two 15min trials separated by ~2h on each testing day. We calculated the number of pellets consumed out of a maximum of 21 per side[306]. Pre-stroke performance was calculated as the average of 4 last trials of training. All post-stroke time point was conducted for 3 days, 2 trials per day, 15 min each separated by ~2h, and the performance was based on the average of all trials. This test assessed fine motor skills of animals and determine the dominant hemisphere by the number of pellets eaten with the contralateral paw.

4.2.8 *In* vivo Drug Penetration Analyses

In order to investigate the *in vivo* release and penetration into the post-stroke brain. 38 Adult male Sprague-Dawley rats, 9-10 weeks of age (Charles River, St. Constant, QC) were used

to perform MCAo procedures for 60 mins each. Subsequent MR imaging was used to assess the size of the stroke one day post-stroke. The 3mm x 5mm duraplasty loaded with 0.33µg EGF and 300 IU EPO were implanted over the removed area at Day 2 during standard DC surgeries as describe as *in vivo* biocompatibility studies. Animals were sacrificed at Day 1 (n=6), Day 2 (n=4), Day 7 (n=3) and Day 14 (n=3) post-implantation. Brain were extracted and placed into the metallic brain matrix slicer (Zivic Instruments, Pittsburgh, PA,). Three 3 mm coronal sectioning sections were obtained from implanted site. Five tissue specimens were dissected as shown in Figure 3. All specimens were then transferred into 2 ml polystyrene microtubes (Thermo Fisher Scientific, Waltham, MA) and snap frozen using dry ice cooled isopropanol. Tubes were stored at -80 °C until analysis.

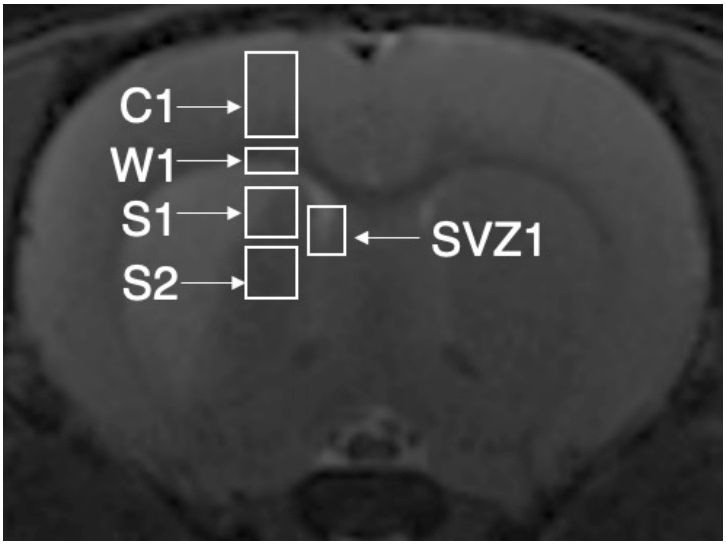

Figure 3. Schematic diagram of the collected location of brain tissue. C1(1.0 mm): Cortex; W1(3.0 mm): White matter; S1(5.0 mm) and S2(7.0 mm): Striatum; SVZ1(6.0 mm): SVZ. Note The size of rectangular frame is only used to define the collected area, not reflect the real size of each harvested issue. The value in bracket represents the estimated distance from implanted site to the collected tissue,

Subsequently, T-PER^{TM} tissue protein extraction reagent (Thermo Fisher Scientific, Waltham, MA) was added to each tube with a total volume of 400 ml. Tissue sections were

homogenized by a plastic drill (Thomas Scientific, Swedesboro, NJ) and tissue fragments were removed by centrifuging homogenized tissue at 15,000 RPM for 15min (Thermo Fisher Scientific, Waltham, MA) at 4°C and the 100 µl homogenate was transferred into 1.5ml Eppendorf tubes. Finally, 200 µl ELISA diluent solution was used to dilute homogenate to a total volume of 300 µl. The amount of protein remaining in the brain homogenate at each time point and site were detected by EGF ELISA kit (Peprotech Inc, Rocky Hill, NJ) as per the manufacturer's instructions.

4.2.9 Statistical Analysis

The results are presented as mean ± standard deviation. All data were treated statistically using ANOVA. A statistically significant difference was considered at $P < 0.05$. Statistical analysis was performed using GraphPad Prism 8 (GraphPad Software, La Jolla, CA).

5. Results and Discussion

5.1 Optimization of fabrication procedure of BBC Duraplasty

The first objective of this project was to optimize the fabrication procedure of the BBC duraplasty developed by our lab. To the current BBC duraplasty fabrication procedure, one purified BC membrane was used to fabricate one lyophilized BBC membrane. The properties of each lyophilized membrane were variable and were difficult to control since the cellulose content of each original purified BC membranes was different. To solve this issue and optimized the yield of lyophilized BBC membranes. We developed a new method that blend all membranes at once to obtain a batch of homogenous cellulose pulp. We assumed that the density of cellulose was constant, the mass of final lyophilized BBC membranes would be positive correlation to the mass of cellulose pulp. We evaluated the relationship of eleven different initial mass of cellulose pulp and their resulted mass of lyophilized BBC membranes in increasing order of cellulose pulp mass

(20g to 70g, 5g increments). Based on the fabrication method, water was the only component that was removed during the filtering and freezing-dry step. There was only one variable factor in the fabrication and hence the collected data was conducted linear regression as shown in Figure 4.

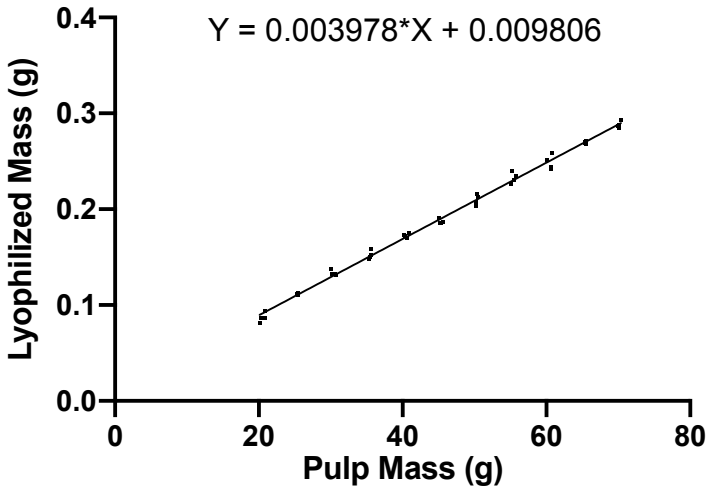

Figure 4. Mass relationship of BBC duraplasty. Mass of cellulose pulp and mass of lyophilized membranes (n=5)

As shown in Figure 4, the regression line was determined: Y=0.003978 * X+0.009806, where X is the mass of pulp and Y is the mass of lyophilized membranes, This equation exhibited the relationship between the initial pulp and final BBC membranes and hence could be used to the further fabrication. The new method and its resulted equation resolve the bigger error in each final BBC membranes. Furthermore, some properties of final production could be adjusted through this method.

5.2 Characterization of BBC Duraplasty

To investigate the characteristic of the BBC duraplasty, six different BBCs of different initial cellulose pulp masses were used: Duraplasty 1 to Duraplasty 6 (data was displayed in Table 4). Swelling ratio (SR) of a hydrogel-like drug delivery platform is an important factor which has remarkable influence on the drug-release performance of the biomaterial[307]. Appropriate

swelling rate is advantageous to the drug diffusion and is usually determined by the pore size and hydrogen bond of biomaterial[308]. As shown in Figure 5, the SR for all BBC duraplasty elevated quickly within the first day and remained almost constant after 96 hours. The SR of duraplasty showed a decreasing trend following the increased mass of BBC duraplasty, where Duraplasty 1 presenting the highest SR and Duraplasty 6 presenting the lowest SR among all samples (Figure 5B). This phenomenon was then identified by SEM and porosity analysis (Figure 5C and D) which is caused by the addition of more cellulose contents will resulted in denser cellulose microstructure and lower porosity (Duraplasty6 is only 13.4±1.2%), therefore weaken the water permeation. It suggests that the initial burst release of drug loaded into the duraplasty can be decreased by the addition of higher cellulose content based on the previous study due to lower porosity[309]. This would be helpful to our application that we are exploring to reduce initial burst to as less as possible. At 96 hours, the highest SR was the lowest cellulose content of 784.060±8.250% (Duraplasty 1) and the lowest one was the highest cellulose content of 527.044±13.015%. It indicated that the SR was decreased with the increased mass of cellulose pulp significantly. Above all, based on the role of SR in drug release performance, the best BBC duraplasty to be a drug-release platform was the Duraplasty6 which is fabricated by 70 grams of cellulose pulp.

Table 4. Different mass of the initial cellulose pulp was used to produce BBC Duraplasty 1-6 and their respective mass of lyophilized membranes: n=5.

Sample	Cellulose Pulp (g)	Lyophilized Cellulose (g)
Duraplasty1	20±0.37085	0.0872±0.00468
Duraplasty2	30±0.27256	0.1336±0.00232
Duraplasty3	40±0.29473	0.1725±0.00248
Duraplasty4	50±0.13647	0.2101±0.00520
Duraplasty5	60±0.24832	0.2491±0.00768
Duraplasty6	70±0.14591	0.2982±0.00349

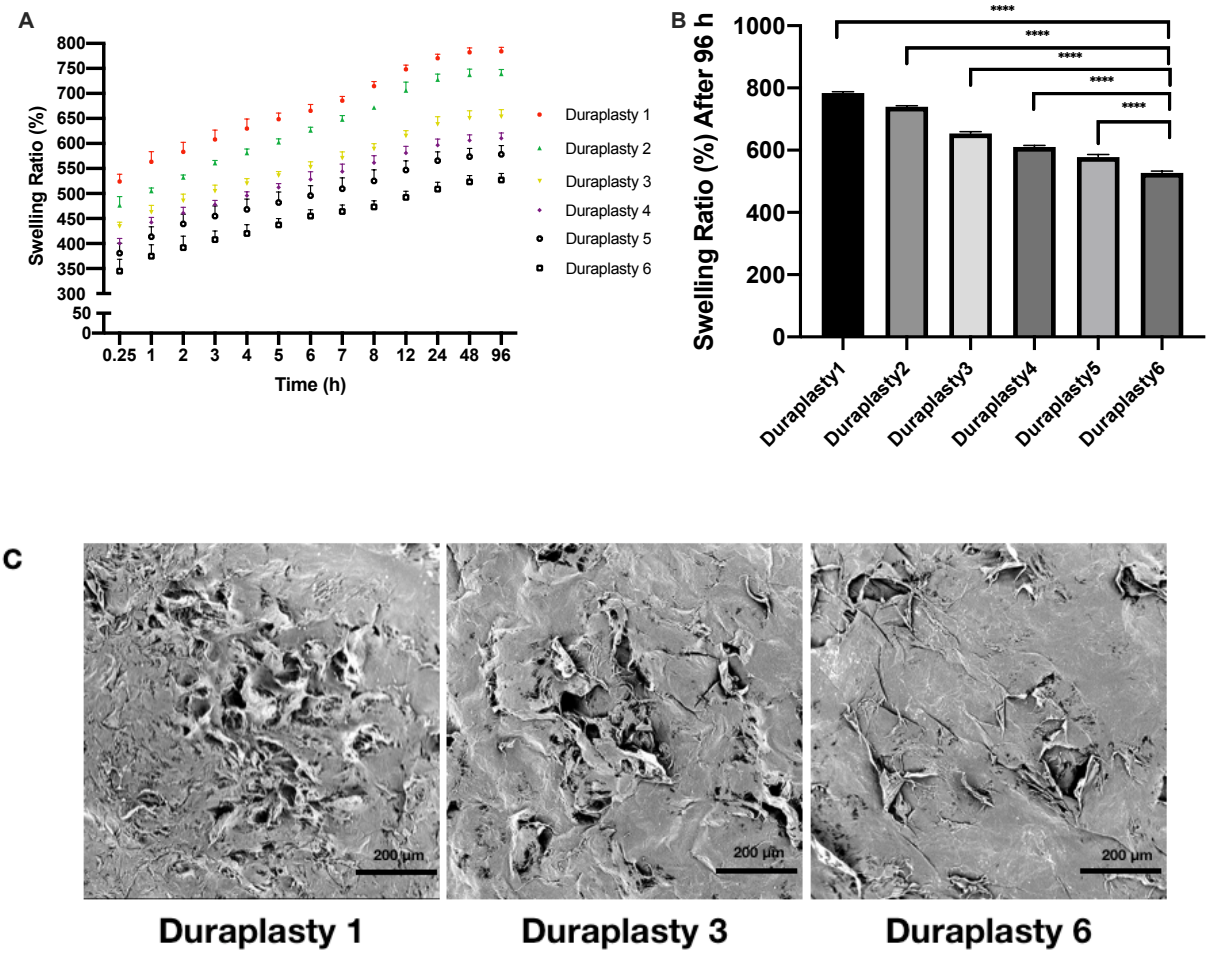
A
Swelling Ratio (%)
800
750
700
650
600
550
500
450
400
350
300
50
0
0.25 1 2 3 4 5 6 7 8 12 24 48 96
Time (h)
Duraplasty 1
Duraplasty 2
Duraplasty 3
Duraplasty 4
Duraplasty 5
Duraplasty 6
B
Swelling Ratio (%) After 96 h
1000
800
600
400
200
0
****
****
****
****
****
Duraplasty1
Duraplasty2
Duraplasty3
Duraplasty4
Duraplasty5
Duraplasty6
C
200 µm
200 µm
200 µm
Duraplasty 1
Duraplasty 3
Duraplasty 6

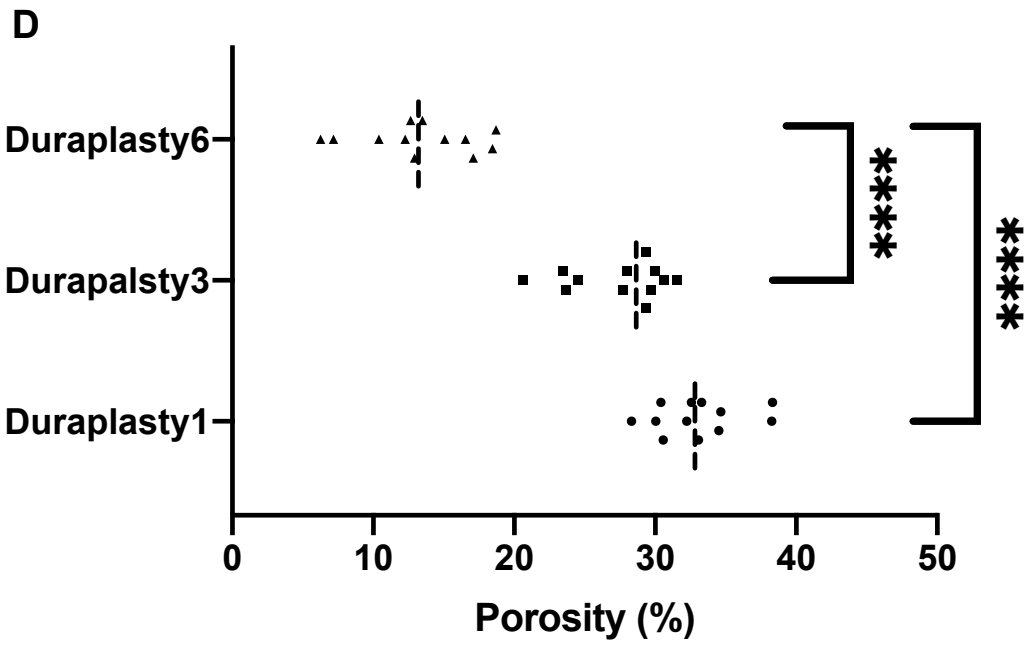

Figure 5. Physical properties of BBC duraplasty. (A) Swelling ratios of Duraplasty 1-6 in PBS at 37°C at different time points, n=8. (B) Swelling ratios of BBC duraplasty after 96 hours. (C) Scanning electron microscopy micrographs of Duraplasty1(20g cellulose pulp), Duraplasty 3(40g cellulose pulp) and Duraplasty6(70g cellulose pulp) with 300x magnification. Fours samples were assayed in duplicate by SEM analysis. (D) Porosity of Duraplasty 1, Duraplasty3, and Duraplasty 6 (One-way ANOVA followed by multiple-comparisons test (Tukey's) was performed for statistical analysis. Data obtained from two independent experiments and presented as mean ± s.e.m.; **$p < 0.01$, ***$p < 0.001$, ****$p < 0.0001$ from Duraplasty 6).

Furthermore, the mechanical properties of duraplasty is also important to the clinical application because it should withstand the manipulation of the implantation procedure after DC. The objective of our plan is using our BBC duraplasty to replace the human dura mater and other synthetic duraplasty, hence the mechanical properties of our BBC duraplasty should be sufficient for surgical handlings[310, 311]. Because of the duraplasty would be infiltrated by CSF once it was implanted to the brain, the duraplasty samples were fully immersed into the PBS solution for

24 hours before test to simulate the real clinical situation. The mechanical properties of the fully rehydrated duraplasty were studied as shown in Figure 6. As excepted, the highest cellulose pulp mass sample-Duraplaty6, demonstrating the strongest Young's Modulus and ultimate tensile strength (UTS) when compared with those duraplasty samples fabricated through less cellulose pulp mass (Duraplasty 1-5). The Young's modulus and UTS of duraplasty6 are 0.288±0.011 MPa and 0.928±0.052 MPa. It is interesting to note that the Young's modulus and UTS of Duraplasty 6 are about 17 times and 8 times higher than Duraplasty 1 (0.017±0.003 MPa and 0.113±0.015 MPa), respectively (Figure 6A and 6B, $p < 0.0001$). As excepted, the highest cellulose pulp mass sample-Duraplaty6, demonstrating the strongest Young's Modulus and ultimate tensile strength (UTS) when compared with those duraplasty samples fabricated through less cellulose pulp mass (Duraplasty 1-5). The Young's modulus and UTS of duraplasty6 are 0.288±0.011 MPa and 0.928 ±0.052 MPa. It is interesting to note that the Young's modulus and UTS of Duraplasty 6 are about 17 times and 8 times higher than Duraplasty 1 (0.017 ± 0.003 MPa and 0.113 ± 0.015 MPa), respectively (Figure 6A and 6B, $p < 0.0001$). These results are consistent with our expectations and are likely because of more cellulose contents can form higher density of hydrogen bonding that lead to the enhanced mechanical properties[312]. In addition, a commercial duraplasty product, Durafrom®, was also tested for its mechanical properties after immersion of PBS for 24 hours. The data of Young's modulus and UTS of Durafrom® were 0.047 ± 0.013 MPa and 0.024 ± 0.014MPa, showing that the mechanical performance of duraplasty fabricated from our lab was stronger than the commercial production through the adjustment of cellulose content.

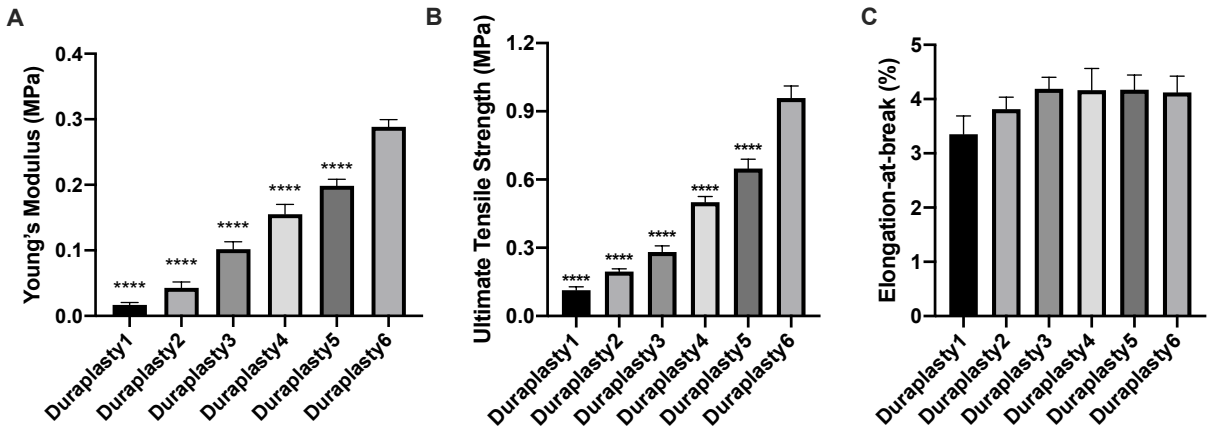

Figure 6. Mechanical properties of BBC duraplasty 1-6. (**A**) Young's Modulus. (**B**) Ultimate tensile strength and (**C**) elongation-at-break of Duraplasty1-6. The mechanical properties were measured using BBC duraplasty samples which were immersed into PBS solution in room temperature 24 hours before test. (One-way ANOVA followed by a multiple-comparisons test (Tukey's) were used for statistical analysis. Data obtained from two independent experiments and is presented as mean ± s.e.m, n = 10. *p < 0.05, ***p < 0.001, ****p < 0.0001 from Duraplasty6).

5.3 Drug Delivery Performance of BBC Duraplasty

The goal of this project is to prepare a BBC duraplasty that incorporate therapeutic drug and that can be implanted as part of a standard DC procedure to enhance functional recoveries of post-stroke brains. Therefore, it is important to evaluate drug release performance of the BBC duraplasty. In this study, because of the less initial burst release, Duraplasty 6 was used for the *in vitro* BSA release study unless indicated otherwise.

To avoid any further negative influences on the post-stoke swollen human brain due to effective pressure, the thickness of Duraplasty6 was measured at the beginning of this study. The thickness of the Duraplasty6 is 0.53 ± 0.02 mm and 1.05 ± 0.13 mm before and after rehydration respectively. The thickness of Duraplasty6 is still under similar range when compared to those human dura maters between 0.53 mm to 1.88 mm even though the thickness of Duraplasty6

doubled after rehydration[313]. Based on this situation, the Duraplasty6 should not be expected to cause any complications when it is implanted to the post-stroke brain.

In this study, BSA was used as a model drug for release study. Specifically, BSA solutions were loaded directly onto the surfaces of Duraplasty6 samples. Through the capillarity of the cellulose network, the BSA solutions were absorbed into the BBC samples.

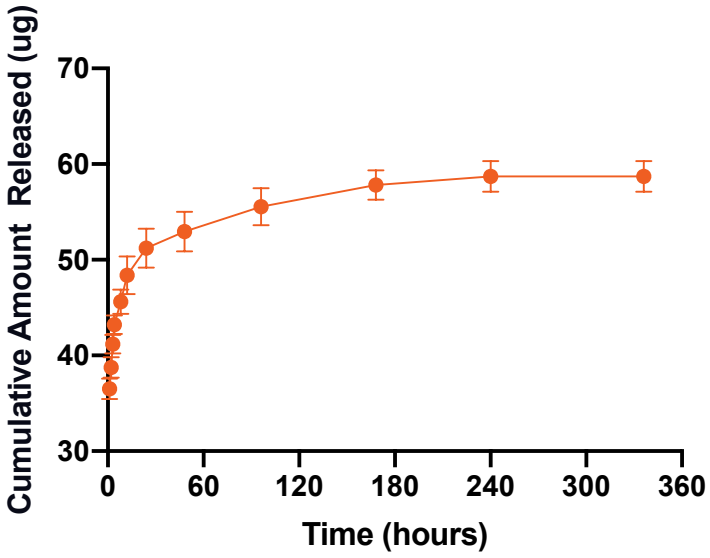

Figure 7. Cumulative release of BSA over 14days as determine by micro BCA protein assay kit, n=6, Data obtained from two independent experiment and presented as mean ± s.e.m

As shown in Figure 7, the BSA-loaded Duraplasty6 showed an initial burst release within the first 8 hours of release (65.18% ± 1.84) and an almost linear release until Day 8. These two phenomena were most likely since the most of BSA molecules were trapped in the outer layers of the Duraplasty and the rest of BSA molecules where in the inner layer were escaped from cellulose structure later. Until the drug release achieve the plateau platform (day 10), 82.85 ± 4.52 % (57.99 ± 3.16 µg) of originally loaded BSA were released from the Duraplasty6 samples. It should be noticed that the activation of endogenous NSPCs after stroke also occur during the similar time

period after stroke[314]. In conclusion, the Duraplasty6 showed the desired release profile which has potential to be a drug delivery platform to the further *in vivo* study.

5.4 *In Vivo* Biocompatibility test of implantation of BBC Duraplasty

To the clinical application, biocompatibility of the implant is mandatory. Hence, we further evaluated our Duraplasty on rats *in vivo* to determine if it is biocompatible and can used on the surface of the brain after DC as shown in Figure 8.

Figure 8. A Euthanized Rat after 4 weeks of DC procedure

Rats were euthanized at 1 week and 4 weeks after DC surgery, the brains of rats were extracted and then the brain coronal sections of rats were used to assessed acute and chronic inflammatory reactions as shown in Figure 9. Samples from both no surgery and DC only group demonstrated the normal histology of the rats' brain. In addition, rat brains with inflammatory reaction which was caused by incident also used to present the pathological phenomena of rejection reaction.

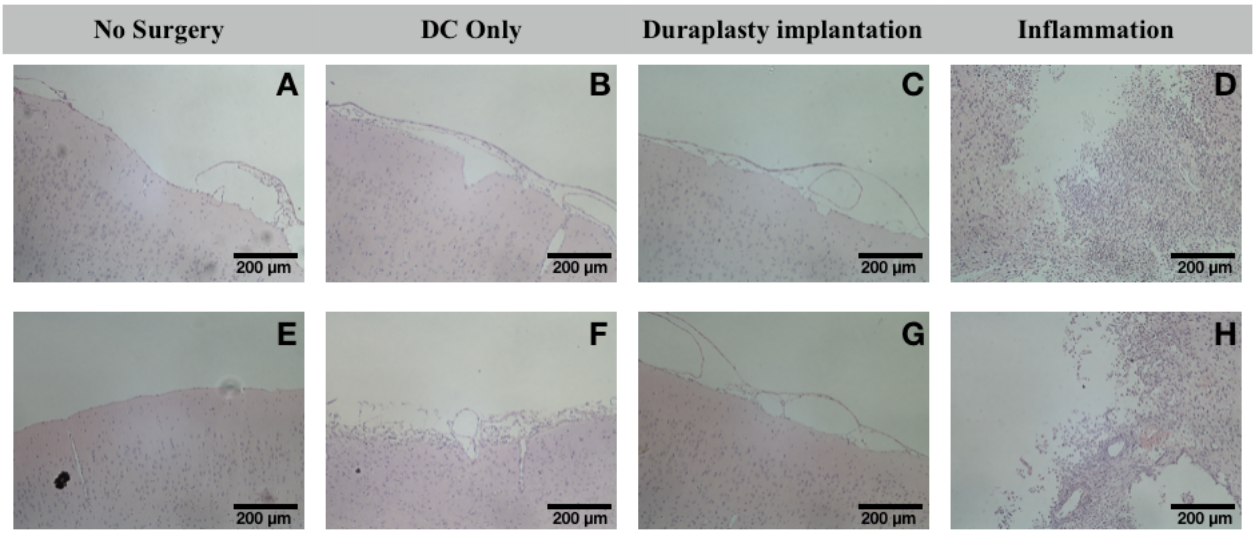

Figure 9. H&E staining of representative coronal brain sections for no surgery and the decompression procedure with or without implantation of BBC Duraplasty, after one and four weeks. Sprague-Dawley brain with (A) No surgery of 1 week, (B) DC only of 1 week, (C) Duraplasty implantation of 1 week, (D) Inflammatory brain of 1 week, (E) No surgery of 4 weeks, (F) DC only of 4 weeks, (G) Duraplasty implantation of 4 weeks, (H) Inflammatory brain of 4 weeks. Note: Duraplasty was removed before sectioning procedure. Images were taken under 10x magnification (scale bar = 200 µm) (N=5).

Compared to the other six images (Figure 9A-B, D-F and H), the images of BBC duraplasty implantation specimens (Figure 9C and G) did not display any appearance of macrophage invasion at the apical surface of the brain for both 1 week and 4 weeks. Also, the neutrophils or eosinophil were not observed, suggesting that no infection and foreign body reaction on the rat brain after the duraplasty implantation at acute and chronic time stage either. The results were consistent to the previous study while implanting the plant-derived cellulose biomaterial subcutaneously[315]. In summary, the above results have provided further evidence to demonstrate that that the BBC duraplasty has excellent *in vivo* compatibility when implanted

5.5 Behavioural assessment following a 60- or 90-minute MCAo time in rats

For our study, in order to simulate the pathological changes of stroke patients, MCAo procedures were carried out on rats to induce strokes. Rats were performed 60 or 90 minutes MCAo procedure (and without any stroke recovery interventions) were assessed for their behavioral performances to establish therapeutic outcome backgrounds. Five behavioral tests: (1) Montoya staircase test; (2) Horizontal-ladder walking test; (3) Cylinder test; (4) Adhesive tape removal tests, and (5) Beam walking test, were performed at each time points as mentioned above. During the surgery, 14 of 26 rats were died during or after surgery within 7 days, the data of incomplete samples were not counted in the analysis.

The Montoya Staircase test was used to assess the independent use in skilled reaching and grasping tasks of forelimbs. As shown in Figure 10, both 60 and 90 min groups achieved a similar number of consumed pellets with their preferred forelimb in baseline. The 60min group consumed 13.04 out of 21 pellets and the 90 min groups is 14.71 out of 21. For the Week 4 of post-stroke surgery, either 60 or 90 min groups reflected a significant decrease ($P < 0.05$) in the mean of consumed pellets through the contralateral forelimb (60 min groups consumed 7.55 pellets and 90 min group is 3.63 pellets). At Week 8, two groups also showed a significant decrease in the pellets consumed of contralateral forelimb. The results are 8.13 of 21 to the 60 min group and 1.56 to the 90 min group ($P < 0.05$). In addition, the significant differences between groups were only found at Week 8 ($P < 0.05$). The results determined that the ability of grasping and reaching has been impaired for both occlusion time group successful through our surgery.

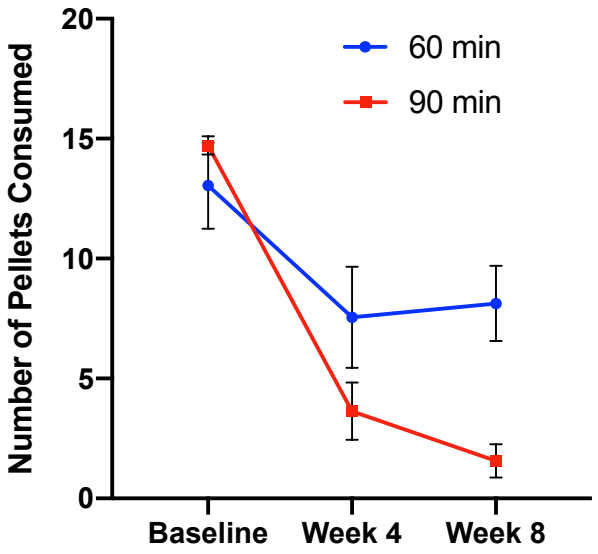

Figure 10. Montoya staircase test, number of pellets consumed of 60 or 90 mins occlusion time groups at each time points (Error bar are mean ± s.e.m, n=6)

The second test is Cylinder test which is used for evaluating locomotor asymmetry in rodent models of CNS disorders and the results as shown in Figure 11. As we can see from Fig 11B, the synergistic utilization of two forelimbs was around 50% of total use before surgery induction and the single use of each paw was fifty-fifty of the rest use. After surgery, both at Week 4 and Week 8, showed a significant decline of the percentage utilization of the impaired paw with a main effect of time as shown in Fig 11A (60 min is 4.033% and 4.303%, 90 min is 6.26% and 5.37% respectively. $P < 0.01$). In addition, the collaboration of two forelimbs after surgery was significant decreased to the 5.43% and 3.16% of 60 min group and 5.09% and 1.94% of 90 min group as well, suggesting that the function of locomotor asymmetry was obvious damaged after the ischemic stroke.

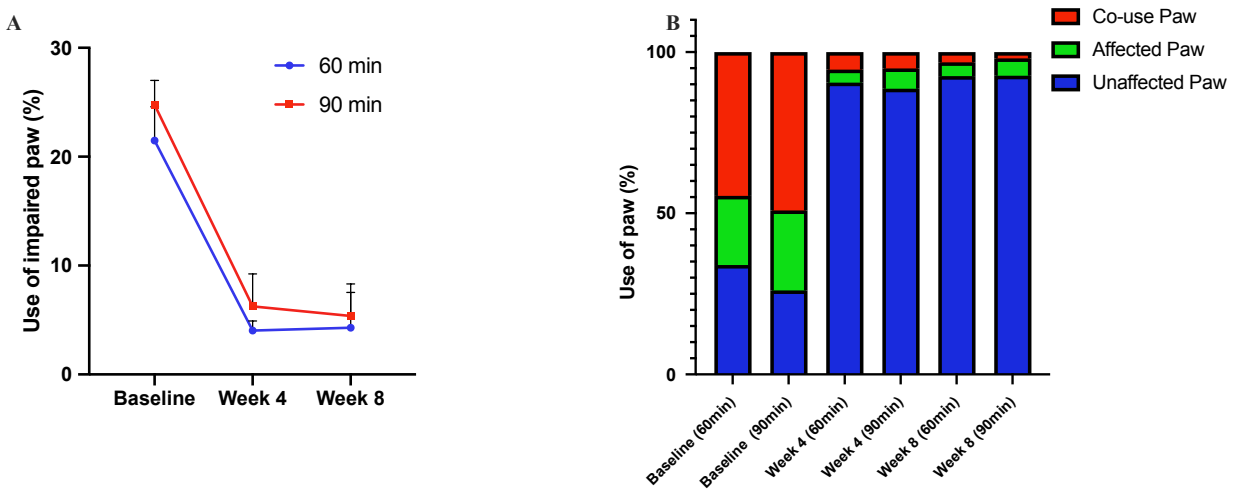

Figure 11. Percentage of each paw use. (A) Percentage of impaired paw at each time points; (B) Percentage distribution of co-use, affected paw, unaffected paw at baseline, week 4 and week 8. （Error bar are mean ± s.e.m, n=6）

To the third test, Beam test, fine motor coordination and balance was used to assess the brain injury after stroke attack as shown in Figure 12. Both forelimb and hindlimb of contralateral side was analyzed to assess the degree of brain damage. As excepted, both two study groups showed equally well during the baseline evaluation (99.59%, 97.13% for 60 min and 99.29%, 98.95% for 90 min). The forelimb of Week 4 and Week 8 showed a decrease in the percentage of successful steps with a main effect of time (60 min: 77.84% and 80.02%; 90 min: 94.90% and 92.27%. $P < 0.05$). In addition, the hindlimb of Week 4 and 8 also showed the similar decline trend of successful steps. Results of Week 4 of 60 min and 90 min groups is 62.15% and 80.73% ($P < 0.05$), also the Week 8 of those two groups was 82.77% and 84.41% respectively. Furthermore, it is noted that the significant differences of successful steps of hindlimb of two groups at Week 4 was found in our study and the 60 min group even performed more impairment of function than the 90 min group ($P < 0.05$).

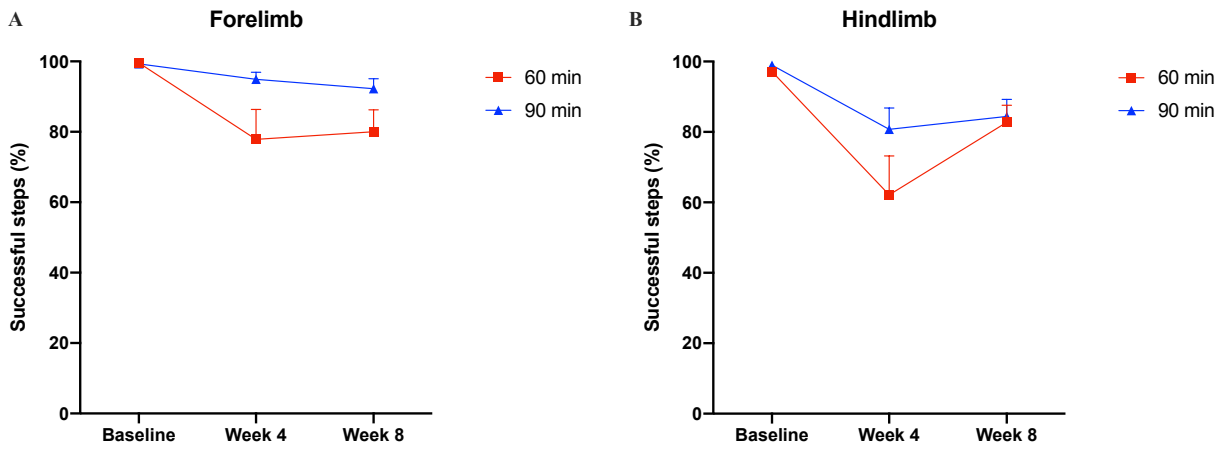

Figure 12. Beam test, percentage of successful steps of impaired forelimb (A) and hindlimb(B) at baseline, week 4 and week 8. （Error bar are mean ± s.e.m, n=6）

Moreover, the next behavioral test is Horizontal-ladder walking test. The percentage of successful steps of injured forelimb and hindlimb was also recorded as well as shown in Figure 13. Both forelimb and hindlimb of two groups showed a significant impairment (60 min: 71.91% and 77.04%; 90 min: 83.80% and 83.99%) at Week 8 ($P < 0.001$). In addition, the significant between-group differences were detected at Week 4 of forelimb and two post-stroke assessment time points of hindlimb ($P < 0.01$). It is worth to note that the behavioral performance of the 60 min group was worse than the 90 min group at both two post-surgery time points in this behavioral test.

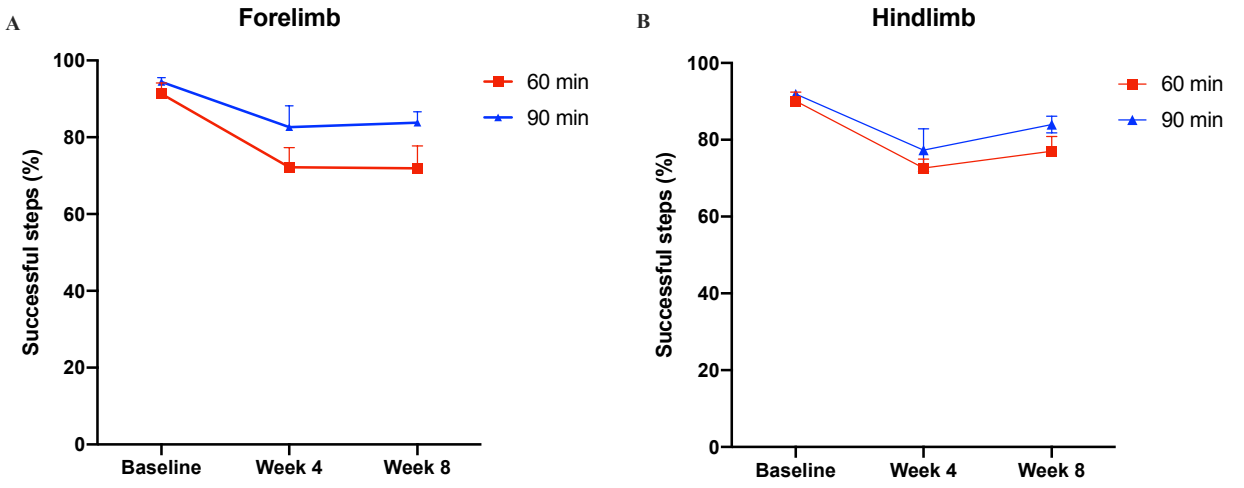

Figure 13. Ladder test. (A) Percentage of successful steps of forelimb; (B) Percentage of successful steps of hindlimb. （Error bar are mean ± s.e.m, n=6）

The last test is Adhesive removal test, the time differences of tape removal between contralateral forelimb and ipsilateral forelimb were analyzed as shown in Figure 14. At all-time points of post stroke, both groups showed a significant increase in time difference between the contralateral and ipsilateral forelimb ($P < 0.01$). To the 60 min occlusion time group, the difference of tape removal test increased from 9.67 to 23.22 seconds at Week 4 and to 60.56 seconds at Week 8. On the other hand, the removal time of 90 min occlusion time was from -9.28 to 34.64 seconds and 47.95 at these two time points respectively. Regarding the group-between significant difference, it was only observed at Week 4 but Week 8 ($P < 0.01$).

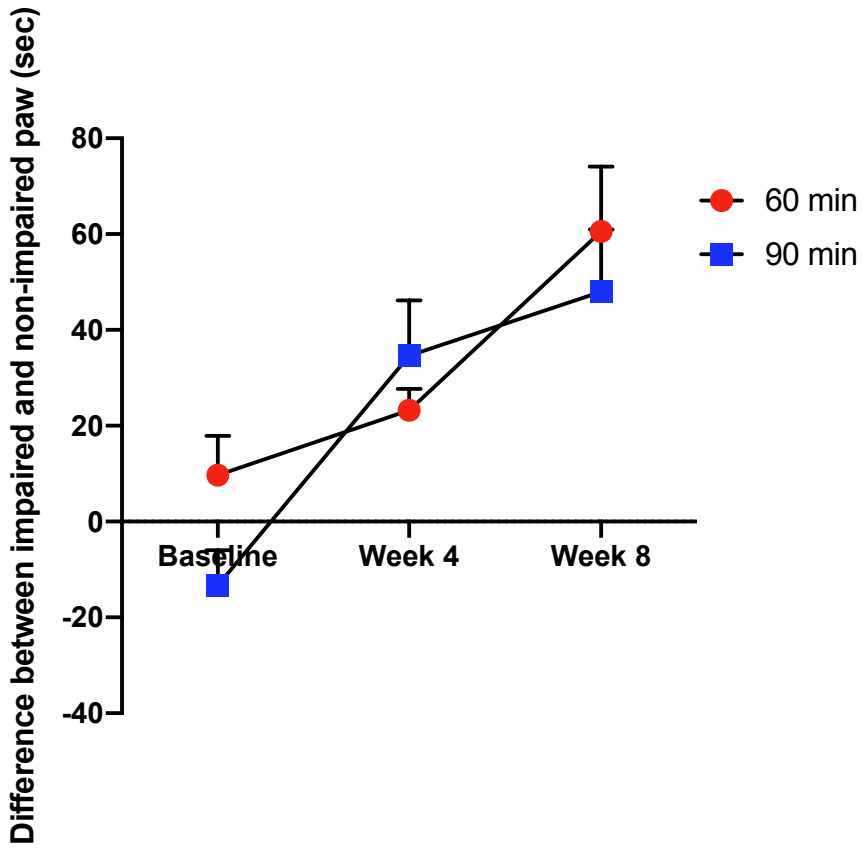

Figure 14. Adhesive removal test. Time differences of tape removal between contralateral forelimb and ipsilateral forelimb at baseline, week 4 and week 8. (Error bar are mean ± s.e.m, n=6)

To the ischemic stroke patients, most of them were affected by the blocking of middle cerebral artery which can lead to severe impairment. Hence, the MCAo rodent stroke model was selected in our study to simulate a similar pathological environment of human patient. The occlusion time of this model is usually a dominant role in the severity of behavioral impairment. The occlusion time over than 90 minutes is always irreversible and be classified as a permanent stroke. The comparison between the 60 and 90 minutes occlusion time will help us to valid the better occlusion time for the following *in vivo* drug penetration study. It will also allow us to know which tests we use will be enough sensitive to be applied on the evaluation of new therapy, showing us significant improvement in function recovery.

During the behavioral studies, we performed above five tests to assess the behavioral differences of rat model between the 60 and 90 minutes MCA occlusion time. Without the consideration of occlusion time, animals in all groups kept impaired for the contralateral forelimb and hindlimb at Week 8 based on these behavioral tests. However, the regularity of results of each test was different once the occlusion time was considered. To the Montoya staircase test, a significant difference between-groups was detected at Week 8 that the 60 minutes occlusion time group was better than the 90 minutes occlusion time. The same behavior was observed for the tape test as well. Rats showed a significant between-group differences at Week 4 but Week 8.

In contrast, both beam and ladder test showed contrary results. A significant between-group difference was only detected at Week 4 of the hindlimb paw in the beam traversal test, with a higher percentage of successful steps for the 90 minute occlusion time group than for the 60 minutes one. Coincidentally, same result was also showed in the ladder test where significant between-groups differences were detected at Week 4 and Week 8 for the forelimb paw and only at Week 8 for the hindlimb. But for both sides, the functional performances of 90 minutes group were better with a higher percentage of successful steps than the 60 minutes groups.

Even though all test excepted cylinder one were found a significant between-groups difference at post-stroke, the variability of results was obvious to each tests. On the one hand, the 60 minutes group obtained a better performance with impaired paw than the 90 minutes one. On the other hand, the 90 minutes group showed a higher score with their impaired paw in the beam and ladder tests. This non-cohesion between tests could come from several reasons. The small sample size may be the main reasons of such results, as 6 rats per groups were not able to perform a precise assessment. Because of the severe brain damage after MCAo surgery, some of rats were dead before post-surgery behavioral test. Only 6 rats of each groups completed the whole tests and

hence the individual result would influence a lot to the overall data. The second factors came from the variability of the lesion size probably. Even though the severity of impairments of brain is mainly caused by the length of occlusion time, the reaction of each sample is different since the diversity of diameter and length of artery. The lesion volume of each brains may vary, and the significant between-groups differences may not able to be detected due to this issue. It will be necessary to reproduce this study with a bigger sample size to allow a possible detection of significant difference between group in the lesion size. For now, the 60-minutes occlusion time was applied to the following study because that it was able to induce significant impairment of motor functions within a shorter period.

5.6 Analysis of *In vivo* EGF penetration

The last study we did is designed to verify the efficacy of BBC duraplasty as a drug delivery system *in vivo*. To detect the change of concentration of EFG and EPO in different area of brain during the time, we implanted the BBC duraplasty loaded with EGF and EPO during the DC procedure at the day 2 of the stroke induction. Rats were euthanized at day 1, 3,7 and 14 after implantation and the brain tissue was collected as described in the methodology section. The mass of tissue was calculated based on the difference of void tube and the tube loaded with tissue. The density of brain was counted as 1.06 g/ml to calculate the volume of brain tissue based on the previous study[316] .

The Human EGF ELISA kit was used to probe the human EGF in the harvested tissue and the results as shown in Figure 15. At 1-day post-implantation (Fig. 15A), the majority of EFG protein was found in C1 and W1 where is around cortical tissue and white matter (C1: 161.4 ng/ml and W1: 130.5 ng/ml). The concentration of S1, S2, SVZ1 is significantly lower than the C1 and W2, the concentration of these three sites is 40.75, 35.02 and 20.89 ng/ml respectively. The results

at 3 days of post-implantation was remarkable, as shown in Fig. 15B, the concentrations of C1, W1, S1, SVZ1 are within 60-90 ng/ml (C1: 72.61 ng/ml; W1: 60.77 ng/ml; S1: 73.41 ng/ml; SVZ1: 93.43 ng/ml). Only site S2 kept the concentration as similar as 1 day of post-implantation (31.98 ng/ml). It is worth to note that the EGF at SVZ1 as well as subventricular zone is detected, which verified our assumption that our BBC duraplasty can deliver bio-active protein to the subventricular zone in the stroke brain after implantation during the DC procedure. To the 7 days and 14 days of post-implantation, the EGF concentration in each site were all maintained low. The concentration of both 7 days and 14 days of five sites are around 10 ng/ml. The main reason of lower concentration was mainly caused by the half-time of protein itself. The half-life of EGF was only 0.74 h in the uninjured brain and 1.69 h in the injured brain, respectively based on the previous study [165]. Hence, some EGF molecules were denatured and then could not be conjugated with ELISA kit after longer time in *in vivo* environment. According to the foregoing research, the suggested recovery therapy period for stroke recovery is to have the release of EGF for the first 7 days and then EPO for the next 7 days[317]. Obviously, the current duraplasty cannot release EGF within an effective concentration up to 7 days to achieve best proliferation outcome of stem cells.

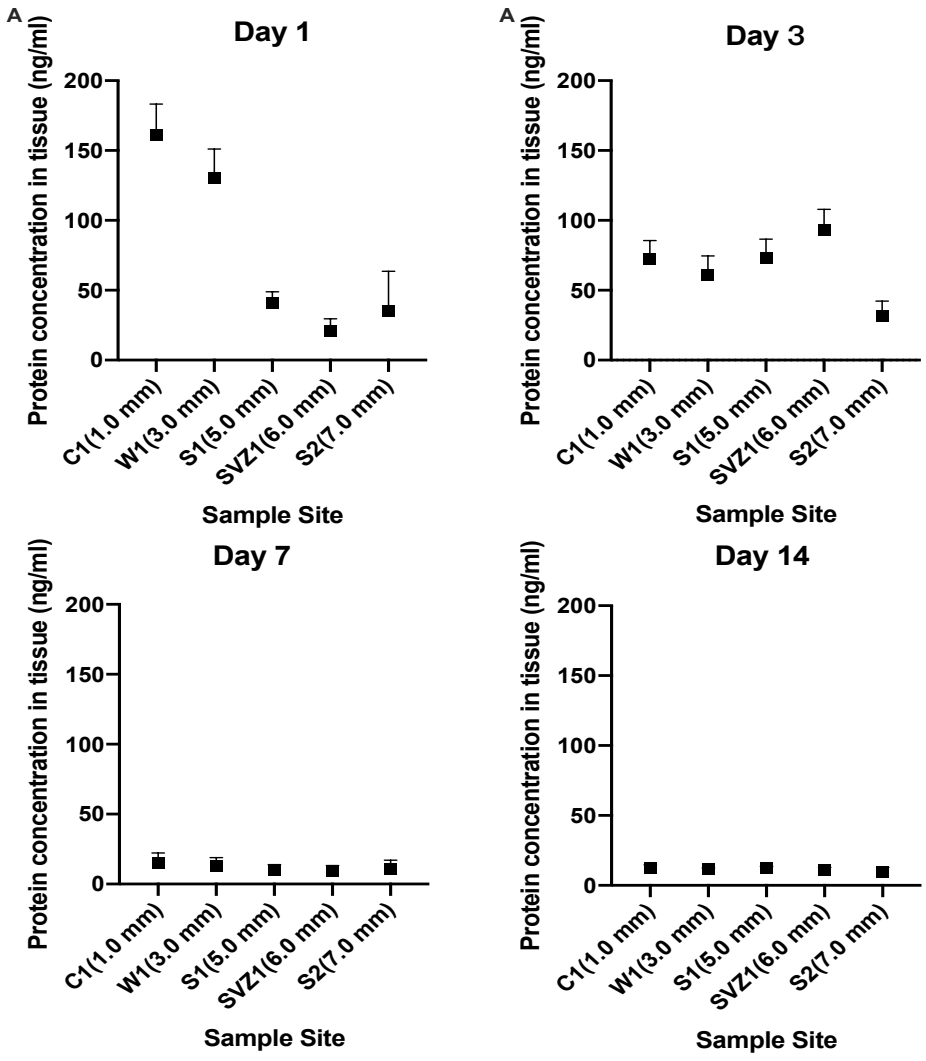

Figure 15. Concentration of human EGF concentration in stroke brains after delivery from implanted BBC duraplasty, the diffusion profiles of EGF at difference site is assessed. (A) At 1 day of post-implantation; (B) At 3 days of post-implantation; (C) At 7 days of post-implantation; (D) At 14 days of post-implantation. (Error bar are mean ± s.e.m)

The above finding suggests that our BBC duraplasty can release the growth factors and then deliver them to the targeted area (SVZ1) at least 3 days after implantation. Although the current BBC duraplasty cannot met the ideal release profile of real stroke recovery therapy since the release profile should match the cells activity period exactly. It is still showing the potential

prospection to be a clinical-applicable duraplasty to replace the traditional commercial duraplasty in the future stroke recovery therapy.

6. Conclusions and Future work

In this article, we determined if the BBC duraplasty that can be implanted as part of DC procedure in stroke patient to delivery growth factors so that they can stimulate neural stem cell proliferation. First, the fabrication procedure of BBC duraplasty was optimized, the mass relationship of BBC between each step was investigated and the equation obtained from data analysis was added to the fabrication procedure as a standard step. The introduction of this equation can control the mass and other parameters of the final duraplasty and hence made the commercialization of BBC duraplasty possible. In addition, the characterization of different BBC duraplasty samples were performed. The series of tests were used to identify the appropriate parameters of BBC duraplasty to be a drug-delivery system. Furthermore, the BSA release profile indicated that the BBC duraplasty can sustained release BSA up to 10 days, confirmed the potential of the BBC duraplasty to be a drug-delivery implant on the stroke recovery. Second, the biocompatibility of the BBC duraplasty was verified. Part of the rat skull was removed and the BBC duraplasty was then implanted over the removed area to mimic the DC procedure performed in the stroke patients. The results of pathological comparison and assessments of each study groups at short-term and long-term (no surgery, DC only, implantation and inflammatory) was promising, The H&E tissue sectioning images of implantation group did not find any obvious inflammatory symptom when compared to the images from DC only and implantation group of brain tissue. In addition, no necrosis and atrophy of brain was detected at both actual and chronic stage as well. The above findings suggest that the BBC duraplasty is *in vivo* biocompatible and can be used as a drug-delivery implant to the further animal study. Furthermore, an appropriate animal stroke

model is a key component of pre-clinical research. The constant stroke pathological environment is necessary otherwise the further *in vivo* drug penetration would not reflect the real distribution and penetration of loaded drug due to the spontaneous recovery. Hence, the ideal occlusion time of MCAo rat model was then studied. The differences of 60 minutes and 90 minutes occlusion time was analyzed through the motor functional performance of five behavioral tests: (1) Montoya Staircase test; (2) Beam traversal test; (3) Ladder rung test; (4) Tape removal test; (5) Cylinder test; The performances and their differences between time and groups were analyzed. All five results confirmed that both 60- and 90-minutes occlusion time length can induce significant motor functional impairment after 4 weeks and 8 weeks of stroke. The motor functional differences of two occlusion times were also compared, only two of five behavioral tests were detected the obvious significant. And, surprise, the beam and ladder test showed the unexpected results that 60 minutes occlusion time groups showed worse performance data compared to the longer time length (90 minutes) at some post-stroke timepoints. Even though the main reason of this situation was caused by the individual variability, to a certain extent, the results suggest that 90 minutes occlusion time would not induce worse motor functional damage to the rats. Based on the results of the pre-trial rat stroke model and the concern of the time cost, we hence selected 60 minutes as the standard occlusion time length to induce stroke in the further *in vivo* study. After the above three antecedent experiments, the feasibility of BBC duraplasty as a drug-loaded implantation has been verified as well as the standard procedure of animal stroke model has been established. We performed *in vivo* protein penetration study in the end of the whole project. This procedure of the experiment was designed to simulate the real circumstances of human stroke patients. Stroke and DC was performed step by step while the BBC duraplasty incorporated with EGF & EPO growth factors was implanted over the swollen brain area. Several pieces of brain tissue from swollen

hemisphere were collected and their supernatant was analyzed through the ELISA kit. The penetration results of day 1 and day 3 of post-implantation was promising that the substantial dose of EGF is existed in the subventricular zone where is the nest of eNSPCs. It provided the higher possibility of stimulation of proliferation and differentiation of those undifferentiated cells, which indicated the idea of BBC drug-loaded duraplasty is viable.

Although the results of above experiments are promising, there are still several works need to be completed. The first one is the development of the dual step releasing drug delivery system. In the current study, only BBC duraplasty was used to be the drug carrier to release and delivery therapeutic molecules. The single stage release profile was not enough for the stimulation of eNSPCs proliferation and differentiation since the time period of these two activities are different. In order to match these time periods, two or more release profiles should be achieved through the multicomponent biomaterial. Therefore, our lab is developing the biodegradable microsphere which can combine with the current BBC duraplasty. We assumed that the multicomponent biomaterial can load and release more than one therapeutic molecule during different time periods. The second matter need to be faced is the appropriate dose of therapeutic molecules. During the above study, we only detected the concentration of EGF in designated area. However, the efficacy of growth factor was not tested such as the performances of neurogenesis and functional recovery after post-implantation. The behavioral assessment of the treatment group needs to be tested to determine if the significant improvement is achieved when compared to the non-treatment group. Also, the differences of neurological environment should be characterized as well through the bromodeoxyuridine or other labeled material. The third issue is the exploration of new therapeutic substance. Currently, we have used the EGF and EPO as the therapeutic drugs to study the recovery of stroke. However, the outcomes of growth factors were limited based on the previous

studies[318]. Therefore, the development of new therapeutic drug is necessary. Exosomes are produced in the endosomal compartment of most eukaryotic cells and it has shown promising potential for the recovery of traumatic brain injury [319]. We are planning to optimize the storage condition of exosomes and then load them to the BBC duraplasty or/and microsphere. We hypothesize that the dual-stage exosome-loaded drug delivery could meet the requirement of stroke recovery and be applied to the human clinical application in the future soon.

Reference

1. Haas, S., N. Weidner, and J. Winkler, *Adult stem cell therapy in stroke.* Current opinion in neurology, 2005. **18**(1): p. 59-64.
2. Obembe, A.O., et al., *Healthcare utilization after stroke in Canada-a population based study.* BMC health services research, 2019. **19**(1): p. 192.
3. Fonarow, G.C., et al., *Timeliness of tissue-type plasminogen activator therapy in acute ischemic stroke: patient characteristics, hospital factors, and outcomes associated with door-to-needle times within 60 minutes.* circulation, 2011. **123**(7): p. 750-758.
4. Yoo, A.J., B. Pulli, and R.G. Gonzalez, *Imaging-based treatment selection for intravenous and intra-arterial stroke therapies: a comprehensive review.* Expert review of cardiovascular therapy, 2011. **9**(7): p. 857-876.
5. Fisher, M. and G.W. Albers, *Advanced imaging to extend the therapeutic time window of acute ischemic stroke.* Annals of neurology, 2013. **73**(1): p. 4-9.
6. Duffis, E.J., et al., *Advanced neuroimaging in acute ischemic stroke: extending the time window for treatment.* Neurosurgical focus, 2011. **30**(6): p. E5.
7. Sandhu, G.S. and J.L. Sunshine, *Advanced neuroimaging to guide acute stroke therapy.* Current cardiology reports, 2012. **14**(6): p. 741-753.
8. Lees, K.R., et al., *Time to treatment with intravenous alteplase and outcome in stroke: an updated pooled analysis of ECASS, ATLANTIS, NINDS, and EPITHET trials.* The Lancet, 2010. **375**(9727): p. 1695-1703.
9. Nih, L.R., S.T. Carmichael, and T. Segura, *Hydrogels for brain repair after stroke: an emerging treatment option.* Current opinion in biotechnology, 2016. **40**: p. 155-163.
10. Nih, L.R., et al., *Injection of microporous annealing particle (MAP) hydrogels in the stroke cavity reduces gliosis and inflammation and promotes NPC migration to the lesion.* Advanced Materials, 2017. **29**(32): p. 1606471.
11. Zhong, J., et al., *Hydrogel matrix to support stem cell survival after brain transplantation in stroke.* Neurorehabilitation and neural repair, 2010. **24**(7): p. 636-644.
12. Bang, O.Y., et al., *Autologous mesenchymal stem cell transplantation in stroke patients.* Annals of Neurology: Official Journal of the American Neurological Association and the Child Neurology Society, 2005. **57**(6): p. 874-882.
13. Reis, C., et al., *A look into stem cell therapy: Exploring the options for treatment of ischemic stroke.* Stem cells international, 2017. **2017**.
14. Buja, L.M. and D. Vela, *Immunologic and inflammatory reactions to exogenous stem cells: implications for experimental studies and clinical trials for myocardial repair.* Journal of the American College of Cardiology, 2010. **56**(21): p. 1693-1700.
15. Meltzer, C.C., et al., *Serial [18F] fluorodeoxyglucose positron emission tomography after human neuronal implantation for stroke.* Neurosurgery, 2001. **49**(3): p. 586-592.
16. Kondziolka, D., et al., *Transplantation of cultured human neuronal cells for patients with stroke.* Neurology, 2000. **55**(4): p. 565-569.
17. Nelson, P.T., et al., *Clonal human (hNT) neuron grafts for stroke therapy: neuropathology in a patient 27 months after implantation.* The American journal of pathology, 2002. **160**(4): p. 1201-1206.
18. Li, Y., et al., *Human marrow stromal cell therapy for stroke in rat: neurotrophins and functional recovery.* neurology, 2002. **59**(4): p. 514-523.

19. Kaneko, N., E. Kako, and K. Sawamoto, *Prospects and limitations of using endogenous neural stem cells for brain regeneration.* Genes, 2011. **2**(1): p. 107-130.
20. Larpthaveesarp, A., D. Ferriero, and F. Gonzalez, *Growth factors for the treatment of ischemic brain injury (growth factor treatment).* Brain sciences, 2015. **5**(2): p. 165-177.
21. Lanfranconi, S., et al., *Growth factors in ischemic stroke.* Journal of cellular and molecular medicine, 2011. **15**(8): p. 1645-1687.
22. Cramer, S.C., *Treatments to promote neural repair after stroke.* Journal of stroke, 2018. **20**(1): p. 57.
23. Talwar, T. and M.V.P. Srivastava, *Role of vascular endothelial growth factor and other growth factors in post-stroke recovery.* Annals of Indian Academy of Neurology, 2014. **17**(1): p. 1.
24. Ashton, R.S., et al., *Scaffolds based on degradable alginate hydrogels and poly (lactide-co-glycolide) microspheres for stem cell culture.* Biomaterials, 2007. **28**(36): p. 5518-5525.
25. Fan, M., et al., *Covalent and injectable chitosan-chondroitin sulfate hydrogels embedded with chitosan microspheres for drug delivery and tissue engineering.* Materials Science and Engineering: C, 2017. **71**: p. 67-74.
26. Caicco, M.J., et al., *A hydrogel composite system for sustained epi-cortical delivery of Cyclosporin A to the brain for treatment of stroke.* Journal of Controlled Release, 2013. **166**(3): p. 197-202.
27. Wan, Y., et al., *Biomimetic synthesis of hydroxyapatite/bacterial cellulose nanocomposites for biomedical applications.* Materials Science and Engineering: C, 2007. **27**(4): p. 855-864.
28. Tuladhar, A., C.M. Morshead, and M.S. Shoichet, *Circumventing the blood–brain barrier: local delivery of cyclosporin A stimulates stem cells in stroke-injured rat brain.* Journal of controlled release, 2015. **215**: p. 1-11.
29. Cook, D.J., et al., *Hydrogel-delivered brain-derived neurotrophic factor promotes tissue repair and recovery after stroke.* Journal of Cerebral Blood Flow & Metabolism, 2017. **37**(3): p. 1030-1045.
30. Traub, M.L., et al., *Oestradiol and insulin-like growth factor-1 reduce cell loss after global ischaemia in middle-aged female rats.* Journal of neuroendocrinology, 2009. **21**(12): p. 1038-1044.
31. Tunkel, A.R. and S.K. Pradhan, *Central nervous system infections in injection drug users.* Infectious disease clinics of North America, 2002. **16**(3): p. 589-605.
32. Meier, U., et al., *Long term outcomes following decompressive craniectomy for severe head injury*, in *Acta Neurochirurgica Supplements*. 2008, Springer. p. 29-31.
33. Carney, N., et al., *Guidelines for the management of severe traumatic brain injury.* Neurosurgery, 2017. **80**(1): p. 6-15.
34. Stevens, R.D., M. Shoykhet, and R. Cadena, *Emergency neurological life support: intracranial hypertension and herniation.* Neurocritical care, 2015. **23**(2): p. 76-82.
35. Broderick, J., et al., *REPRINT: Guidelines for the Management of Spontaneous Intracerebral Hemorrhage in Adults: 2007 Update: A Guideline From the American Heart Association/American Stroke Association Stroke Council, High Blood Pressure Research Council, and the Quality of Care and Outcomes in Research Interdisciplinary Working Group: The American Academy of Neurology affirms the value of this guideline as an educational tool for neurologists.* Circulation, 2007. **116**(16): p. e391-e413.

36. Shah, S. and W.T. Kimberly. *Today's approach to treating brain swelling in the neuro intensive care unit*. in *Seminars in neurology*. 2016. Thieme Medical Publishers.
37. Sokolnicki, A.M., et al., *Permeability of bacterial cellulose membranes.* Journal of membrane science, 2006. **272**(1-2): p. 15-27.
38. Moosavi-Nasab, M. and A.R. Yousefi, *Investigation of physicochemical properties of the bacterial cellulose produced by Gluconacetobacter xylinus from date syrup.* World Academy of Science, Engineering and Technology, 2010. **44**: p. 1258-1263.
39. Barud, H.S., et al., *Kinetic parameters for thermal decomposition of microcrystalline, vegetal, and bacterial cellulose.* Journal of thermal analysis and calorimetry, 2011. **105**(2): p. 421-426.
40. Lin, S.-P., et al., *Biosynthesis, production and applications of bacterial cellulose.* Cellulose, 2013. **20**(5): p. 2191-2219.
41. Choi, C.N., et al., *Properties of bacterial cellulose produced in a pilot-scale spherical type bubble column bioreactor.* Korean Journal of Chemical Engineering, 2009. **26**(1): p. 136.
42. Ul-Islam, M., T. Khan, and J.K. Park, *Water holding and release properties of bacterial cellulose obtained by in situ and ex situ modification.* Carbohydrate Polymers, 2012. **88**(2): p. 596-603.
43. Wan, Y., et al., *Preparation and characterization of bacterial cellulose/heparin hybrid nanofiber for potential vascular tissue engineering scaffolds.* Polymers for Advanced Technologies, 2011. **22**(12): p. 2643-2648.
44. Xiong, G., et al., *A novel in vitro three-dimensional macroporous scaffolds from bacterial cellulose for culture of breast cancer cells.* Journal of Biomaterials and Nanobiotechnology, 2013. **4**(04): p. 316.
45. Hu, W., et al., *Functionalized bacterial cellulose derivatives and nanocomposites.* Carbohydrate polymers, 2014. **101**: p. 1043-1060.
46. Koike, T., et al., *Efficacy of Bacterial Cellulose as a Carrier of BMP-2 for Bone Regeneration in a Rabbit Frontal Sinus Model.* Materials, 2019. **12**(15): p. 2489.
47. Sukul, M., et al., *Effect of local sustainable release of BMP2-VEGF from nano-cellulose loaded in sponge biphasic calcium phosphate on bone regeneration.* Tissue Engineering Part A, 2015. **21**(11-12): p. 1822-1836.
48. Pelling, A.E. and R.J. Hickey, *Cellulose biomaterials for tissue engineering.* Frontiers in Bioengineering and Biotechnology, 2019. **7**: p. 45.
49. Muselík, J., et al., *Evaluation of the influence of sterilization method on the stability of carboxymethyl cellulose wound dressing.* Ceska a Slovenska farmacie: casopis Ceske farmaceuticke spolecnosti a Slovenske farmaceuticke spolecnosti, 2013. **62**(2): p. 95-98.
50. Rnjak-Kovacina, J., et al., *The effect of sterilization on silk fibroin biomaterial properties.* Macromolecular bioscience, 2015. **15**(6): p. 861-874.
51. Dai, Z., et al., *Sterilization techniques for biodegradable scaffolds in tissue engineering applications.* Journal of tissue engineering, 2016. **7**: p. 2041731416648810.
52. Katan, M. and A. Luft. *Global burden of stroke*. in *Seminars in neurology*. 2018. Thieme Medical Publishers.
53. Flynn, R., R. MacWalter, and A. Doney, *The cost of cerebral ischaemia.* Neuropharmacology, 2008. **55**(3): p. 250-256.
54. Dirnagl, U., C. Iadecola, and M.A. Moskowitz, *Pathobiology of ischaemic stroke: an integrated view.* Trends in neurosciences, 1999. **22**(9): p. 391-397.

55. Morgenstern, L.B., et al., *Guidelines for the management of spontaneous intracerebral hemorrhage: a guideline for healthcare professionals from the American Heart Association/American Stroke Association.* Stroke, 2010. **41**(9): p. 2108-2129.
56. Fisher, M., et al., *Toward a multimodal neuroprotective treatment of stroke.* Stroke, 2006. **37**(4): p. 1129-1136.
57. Tam, R.Y., et al., *Regenerative therapies for central nervous system diseases: a biomaterials approach.* Neuropsychopharmacology, 2014. **39**(1): p. 169.
58. Sensharma, P., et al., *Biomaterials and cells for neural tissue engineering: Current choices.* Materials Science and Engineering: C, 2017. **77**: p. 1302-1315.
59. Von Kummer, R., et al., *Acute stroke: usefulness of early CT findings before thrombolytic therapy.* Radiology, 1997. **205**(2): p. 327-333.
60. ATLANTIS, T., *Association of outcome with early stroke treatment: pooled analysis of ATLANTIS, ECASS, and NINDS rt-PA stroke trials.* The Lancet, 2004. **363**(9411): p. 768-774.
61. Kwiatkowski, T.G., et al., *Effects of tissue plasminogen activator for acute ischemic stroke at one year.* New England Journal of Medicine, 1999. **340**(23): p. 1781-1787.
62. Hacke, W., et al., *Thrombolysis with alteplase 3 to 4.5 hours after acute ischemic stroke.* New England journal of medicine, 2008. **359**(13): p. 1317-1329.
63. Pan, J., et al., *Reperfusion injury following cerebral ischemia: pathophysiology, MR imaging, and potential therapies.* Neuroradiology, 2007. **49**(2): p. 93-102.
64. Saver, J.L., et al., *Stent-retriever thrombectomy after intravenous t-PA vs. t-PA alone in stroke.* New England Journal of Medicine, 2015. **372**(24): p. 2285-2295.
65. Lindvall, O., Z. Kokaia, and A. Martinez-Serrano, *Stem cell therapy for human neurodegenerative disorders–how to make it work.* Nature medicine, 2004. **10**(7s): p. S42.
66. Tuch, B.E., *Stem cells: a clinical update.* Australian family physician, 2006. **35**(9): p. 719.
67. Meyers, P.M., et al., *Current status of endovascular stroke treatment.* Circulation, 2011. **123**(22): p. 2591-2601.
68. Parker, G.C., *Stem cell therapy for stroke.* Journal of Pediatric Neurology, 2010. **8**(03): p. 333-341.
69. Zhao, L.-R., et al., *Human bone marrow stem cells exhibit neural phenotypes and ameliorate neurological deficits after grafting into the ischemic brain of rats.* Experimental neurology, 2002. **174**(1): p. 11-20.
70. Lee, J.S., et al., *A long-term follow-up study of intravenous autologous mesenchymal stem cell transplantation in patients with ischemic stroke.* Stem cells, 2010. **28**(6): p. 1099-1106.
71. Zheng, H., et al., *Mesenchymal Stem Cell Therapy in Stroke: A Systematic Review of Literature in Pre-Clinical and Clinical Research.* Cell transplantation, 2018. **27**(12): p. 1723-1730.
72. Wright, L.S., et al., *Human progenitor cells isolated from the developing cortex undergo decreased neurogenesis and eventual senescence following expansion in vitro.* Experimental cell research, 2006. **312**(11): p. 2107-2120.
73. Svendsen, C., et al., *Survival and differentiation of rat and human epidermal growth factor-responsive precursor cells following grafting into the lesioned adult central nervous system.* Experimental neurology, 1996. **137**(2): p. 376-388.
74. Xin, Z.-C., et al., *Recruiting endogenous stem cells: a novel therapeutic approach for erectile dysfunction.* Asian journal of andrology, 2016. **18**(1): p. 10.

75. Kuhn, H.G., H. Dickinson-Anson, and F.H. Gage, *Neurogenesis in the dentate gyrus of the adult rat: age-related decrease of neuronal progenitor proliferation.* Journal of Neuroscience, 1996. **16**(6): p. 2027-2033.
76. Eriksson, P.S., et al., *Neurogenesis in the adult human hippocampus.* Nature medicine, 1998. **4**(11): p. 1313.
77. Kaplan, M.S. and D.H. Bell, *Mitotic neuroblasts in the 9-day-old and 11-month-old rodent hippocampus.* Journal of Neuroscience, 1984. **4**(6): p. 1429-1441.
78. Altman, J. and G.D. Das, *Autoradiographic and histological evidence of postnatal hippocampal neurogenesis in rats.* Journal of Comparative Neurology, 1965. **124**(3): p. 319-335.
79. Sanai, N., et al., *Unique astrocyte ribbon in adult human brain contains neural stem cells but lacks chain migration.* Nature, 2004. **427**(6976): p. 740.
80. Arvidsson, A., et al., *Neuronal replacement from endogenous precursors in the adult brain after stroke.* Nature medicine, 2002. **8**(9): p. 963.
81. Zhang, R., et al., *Activated neural stem cells contribute to stroke-induced neurogenesis and neuroblast migration toward the infarct boundary in adult rats.* Journal of Cerebral Blood Flow & Metabolism, 2004. **24**(4): p. 441-448.
82. Zhang, R., et al., *Stroke transiently increases subventricular zone cell division from asymmetric to symmetric and increases neuronal differentiation in the adult rat.* Journal of Neuroscience, 2004. **24**(25): p. 5810-5815.
83. Arvidsson, A., Z. Kokaia, and O. Lindvall, *N-methyl-D-aspartate receptor-mediated increase of neurogenesis in adult rat dentate gyrus following stroke.* European Journal of Neuroscience, 2001. **14**(1): p. 10-18.
84. Rice, A., et al., *Proliferation and neuronal differentiation of mitotically active cells following traumatic brain injury.* Experimental neurology, 2003. **183**(2): p. 406-417.
85. Parent, J.M., et al., *Rat forebrain neurogenesis and striatal neuron replacement after focal stroke.* Annals of Neurology: Official Journal of the American Neurological Association and the Child Neurology Society, 2002. **52**(6): p. 802-813.
86. Sun, Y., et al., *VEGF-induced neuroprotection, neurogenesis, and angiogenesis after focal cerebral ischemia.* The Journal of clinical investigation, 2003. **111**(12): p. 1843-1851.
87. Jiang, W., et al., *Cortical neurogenesis in adult rats after transient middle cerebral artery occlusion.* Stroke, 2001. **32**(5): p. 1201-1207.
88. Teramoto, T., et al., *EGF amplifies the replacement of parvalbumin-expressing striatal interneurons after ischemia.* The Journal of clinical investigation, 2003. **111**(8): p. 1125-1132.
89. Jin, K., et al., *Stem cell factor stimulates neurogenesis in vitro and in vivo.* The Journal of clinical investigation, 2002. **110**(3): p. 311-319.
90. Kuhn, H.G., et al., *Epidermal growth factor and fibroblast growth factor-2 have different effects on neural progenitors in the adult rat brain.* Journal of Neuroscience, 1997. **17**(15): p. 5820-5829.
91. Yoshimura, S., et al., *FGF-2 regulation of neurogenesis in adult hippocampus after brain injury.* Proceedings of the National Academy of Sciences, 2001. **98**(10): p. 5874-5879.
92. Jin, K., et al., *Vascular endothelial growth factor (VEGF) stimulates neurogenesis in vitro and in vivo.* Proceedings of the National Academy of Sciences, 2002. **99**(18): p. 11946-11950.

93. Schänzer, A., et al., *Direct stimulation of adult neural stem cells in vitro and neurogenesis in vivo by vascular endothelial growth factor.* Brain pathology, 2004. **14**(3): p. 237-248.
94. Shingo, T., et al., *Erythropoietin regulates the in vitro and in vivo production of neuronal progenitors by mammalian forebrain neural stem cells.* Journal of Neuroscience, 2001. **21**(24): p. 9733-9743.
95. Gustafsson, E., et al., *Anterograde delivery of brain‐derived neurotrophic factor to striatum via nigral transduction of recombinant adeno‐associated virus increases neuronal death but promotes neurogenic response following stroke.* European Journal of Neuroscience, 2003. **17**(12): p. 2667-2678.
96. Chmielnicki, E., et al., *Adenovirally expressed noggin and brain-derived neurotrophic factor cooperate to induce new medium spiny neurons from resident progenitor cells in the adult striatal ventricular zone.* Journal of Neuroscience, 2004. **24**(9): p. 2133-2142.
97. Zhang, H., et al., *VEGF is a chemoattractant for FGF-2–stimulated neural progenitors.* The Journal of cell biology, 2003. **163**(6): p. 1375-1384.
98. Nakatomi, H., et al., *Regeneration of hippocampal pyramidal neurons after ischemic brain injury by recruitment of endogenous neural progenitors.* Cell, 2002. **110**(4): p. 429-441.
99. Wang, L., et al., *Treatment of stroke with erythropoietin enhances neurogenesis and angiogenesis and improves neurological function in rats.* Stroke, 2004. **35**(7): p. 1732-1737.
100. Arnaout, O.M., et al., *Decompressive hemicraniectomy after malignant middle cerebral artery infarction: rationale and controversies.* Neurosurgical focus, 2011. **30**(6): p. E18.
101. Staykov, D. and R. Gupta, *Hemicraniectomy in malignant middle cerebral artery infarction.* Stroke, 2011. **42**(2): p. 513-516.
102. Jüttler, E., et al., *Hemicraniectomy in older patients with extensive middle-cerebral-artery stroke.* New England Journal of Medicine, 2014. **370**(12): p. 1091-1100.
103. Doerfler, A., et al., *Decompressive craniectomy in a rat model of "malignant" cerebral hemispheric stroke: experimental support for an aggressive therapeutic approach.* Journal of neurosurgery, 1996. **85**(5): p. 853-859.
104. Murthy, J., et al., *Decompressive craniectomy with clot evacuation in large hemispheric hypertensive intracerebral hemorrhage.* Neurocritical care, 2005. **2**(3): p. 258-262.
105. Harscher, S., et al., *Outcome after decompressive craniectomy in patients with severe ischemic stroke.* Acta neurochirurgica, 2006. **148**(1): p. 31-37.
106. Vahedi, K., et al., *Sequential-design, multicenter, randomized, controlled trial of early decompressive craniectomy in malignant middle cerebral artery infarction (DECIMAL Trial).* Stroke, 2007. **38**(9): p. 2506-2517.
107. Lu, X., et al., *Decompressive craniectomy for the treatment of malignant infarction of the middle cerebral artery.* Scientific reports, 2014. **4**: p. 7070.
108. Abbott, N.J., L. Rönnbäck, and E. Hansson, *Astrocyte–endothelial interactions at the blood–brain barrier.* Nature reviews neuroscience, 2006. **7**(1): p. 41.
109. Stamatovic, S.M., R.F. Keep, and A.V. Andjelkovic, *Brain endothelial cell-cell junctions: how to "open" the blood brain barrier.* Current neuropharmacology, 2008. **6**(3): p. 179-192.
110. Pardridge, W.M., *The blood-brain barrier: bottleneck in brain drug development.* NeuroRx, 2005. **2**(1): p. 3-14.
111. Brownlees, J. and C. Williams, *Peptidases, peptides, and the mammalian blood–brain barrier.* Journal of neurochemistry, 1993. **60**(3): p. 793-803.

112. Yoon, J.H., et al., *Local delivery of nitric oxide from an eluting stent to inhibit neointimal thickening in a porcine coronary injury model.* Yonsei medical journal, 2002. **43**(2): p. 242-251.
113. Wang, P.P., J. Frazier, and H. Brem, *Local drug delivery to the brain.* Advanced drug delivery reviews, 2002. **54**(7): p. 987-1013.
114. Ulapane, K.R., et al., *Improving brain delivery of biomolecules via BBB modulation in mouse and rat: Detection using MRI, NIRF, and mass spectrometry.* Nanotheranostics, 2017. **1**(2): p. 217.
115. Teocchi, M.A., *Modelos animais no estudo de AVC.* ComCiência, 2009(109): p. 0-0.
116. Bogousslavsky, J., G. Van Melle, and F. Regli, *The Lausanne Stroke Registry: analysis of 1,000 consecutive patients with first stroke.* Stroke, 1988. **19**(9): p. 1083-1092.
117. Koizumi, J., *Experimental studies of ischemic brain edema. 1. A new experimental model of cerebral embolism in rats in which recirculation can be introduced in the ischemic area.* Jpn J stroke, 1986. **8**: p. 1-8.
118. Longa, E.Z., et al., *Reversible middle cerebral artery occlusion without craniectomy in rats.* stroke, 1989. **20**(1): p. 84-91.
119. Tamura, A., et al., *Focal cerebral ischaemia in the rat: 1. Description of technique and early neuropathological consequences following middle cerebral artery occlusion.* Journal of Cerebral Blood Flow & Metabolism, 1981. **1**(1): p. 53-60.
120. Howells, D.W., et al., *Different strokes for different folks: the rich diversity of animal models of focal cerebral ischemia.* Journal of Cerebral Blood Flow & Metabolism, 2010. **30**(8): p. 1412-1431.
121. McAuley, M., *Rodent models of focal ischemia.* Cerebrovascular and brain metabolism reviews, 1995. **7**(2): p. 153-180.
122. Yanamoto, H., et al., *Evaluation of MCAO stroke models in normotensive rats: standardized neocortical infarction by the 3VO technique.* Experimental neurology, 2003. **182**(2): p. 261-274.
123. Buchan, A.M., D. Xue, and A. Slivka, *A new model of temporary focal neocortical ischemia in the rat.* Stroke, 1992. **23**(2): p. 273-279.
124. Watson, B.D., et al., *Induction of reproducible brain infarction by photochemically initiated thrombosis.* Annals of Neurology: Official Journal of the American Neurological Association and the Child Neurology Society, 1985. **17**(5): p. 497-504.
125. Kuroiwa, T., et al., *Development of a rat model of photothrombotic ischemia and infarction within the caudoputamen.* Stroke, 2009. **40**(1): p. 248-253.
126. Lee, V.M., et al., *Evolution of photochemically induced focal cerebral ischemia in the rat. Magnetic resonance imaging and histology.* Stroke, 1996. **27**(11): p. 2110-8; discussion 2118-9.
127. Provenzale, J.M., et al., *Assessment of the patient with hyperacute stroke: imaging and therapy.* Radiology, 2003. **229**(2): p. 347-359.
128. Harrison, T.C., et al., *Displacement of sensory maps and disorganization of motor cortex after targeted stroke in mice.* Stroke, 2013. **44**(8): p. 2300-2306.
129. Yanagisawa, M., et al., *A novel peptide vasoconstrictor, endothelin, is produced by vascular endothelium and modulates smooth muscle Ca2+ channels.* Journal of hypertension. Supplement: official journal of the International Society of Hypertension, 1988. **6**(4): p. S188-91.

130. Sharkey, J., *Perivascular microapplication of endothelin-1: a new model of focal cerebral ischaemia in the rat.* Journal of Cerebral Blood Flow & Metabolism, 1993. **13**(5): p. 865-871.
131. Fuxe, K., et al., *Endothelin-1 induced lesions of the frontoparietal cortex of the rat. A possible model of focal cortical ischemia.* Neuroreport, 1997. **8**(11): p. 2623-2629.
132. Hossmann, K.-A., *Cerebral ischemia: models, methods and outcomes.* Neuropharmacology, 2008. **55**(3): p. 257-270.
133. Rapp, J.H., et al., *Microemboli composed of cholesterol crystals disrupt the blood-brain barrier and reduce cognition.* Stroke, 2008. **39**(8): p. 2354-2361.
134. Wang, C.X., et al., *Patency of cerebral microvessels after focal embolic stroke in the rat.* Journal of Cerebral Blood Flow & Metabolism, 2001. **21**(4): p. 413-421.
135. Smith, W.S., et al., *Safety and efficacy of mechanical embolectomy in acute ischemic stroke: results of the MERCI trial.* Stroke, 2005. **36**(7): p. 1432-1438.
136. Liu, S., et al., *Rodent stroke model guidelines for preclinical stroke trials.* Journal of experimental stroke & translational medicine, 2009. **2**(2): p. 2.
137. Schmid-Elsaesser, R., et al., *A critical reevaluation of the intraluminal thread model of focal cerebral ischemia.* Stroke, 1998. **29**(10): p. 2162-70.
138. Garcia, J.H., K.-F. Liu, and K.-L. Ho, *Neuronal necrosis after middle cerebral artery occlusion in Wistar rats progresses at different time intervals in the caudoputamen and the cortex.* Stroke, 1995. **26**(4): p. 636-643.
139. Maeda, K., R. Hata, and K.-A. Hossmann, *Regional metabolic disturbances and cerebrovascular anatomy after permanent middle cerebral artery occlusion in C57black/6 and SV129 mice.* Neurobiology of disease, 1999. **6**(2): p. 101-108.
140. McColl, B.W., et al., *Extension of cerebral hypoperfusion and ischaemic pathology beyond MCA territory after intraluminal filament occlusion in C57Bl/6J mice.* Brain research, 2004. **997**(1): p. 15-23.
141. Türeyen, K., et al., *Ideal suture diameter is critical for consistent middle cerebral artery occlusion in mice.* Operative Neurosurgery, 2005. **56**(suppl_1): p. ONS-196-ONS-200.
142. Zarow, G., et al., *Endovascular suture occlusion of the middle cerebral artery in rats: effect of suture insertion distance on cerebral blood flow, infarct distribution and infarct volume.* Neurological research, 1997. **19**(4): p. 409-416.
143. Bouley, J., M. Fisher, and N. Henninger, *Comparison between coated vs. uncoated suture middle cerebral artery occlusion in the rat as assessed by perfusion/diffusion weighted imaging.* Neuroscience letters, 2007. **412**(3): p. 185-190.
144. Belayev, L., et al., *Quantitative evaluation of blood-brain barrier permeability following middle cerebral artery occlusion in rats.* Brain research, 1996. **739**(1-2): p. 88-96.
145. Dietrich, W.D., et al., *Photochemically induced cortical infarction in the rat. 1. Time course of hemodynamic consequences.* Journal of Cerebral Blood Flow & Metabolism, 1986. **6**(2): p. 184-194.
146. Hughes, P., et al., *Focal lesions in the rat central nervous system induced by endothelin-1.* Journal of Neuropathology & Experimental Neurology, 2003. **62**(12): p. 1276-1286.
147. Robinson, M., et al., *Reduction of local cerebral blood flow to pathological levels by endothelin-1 applied to the middle cerebral artery in the rat.* Neuroscience letters, 1990. **118**(2): p. 269-272.
148. Biernaskie, J., et al., *A serial MR study of cerebral blood flow changes and lesion development following endothelin-1-induced ischemia in rats.* Magnetic Resonance in

Medicine: An Official Journal of the International Society for Magnetic Resonance in Medicine, 2001. **46**(4): p. 827-830.
149. Hung, V.K., et al., *Selective astrocytic endothelin-1 overexpression contributes to dementia associated with ischemic stroke by exaggerating astrocyte-derived amyloid secretion.* Journal of Cerebral Blood Flow & Metabolism, 2015. **35**(10): p. 1687-1696.
150. Uesugi, M., et al., *SB209670, a potent endothelin receptor antagonist, prevents or delays axonal degeneration after spinal cord injury.* Brain research, 1998. **786**(1-2): p. 235-239.
151. Carmichael, S.T., *Rodent models of focal stroke: size, mechanism, and purpose.* NeuroRx, 2005. **2**(3): p. 396-409.
152. Gerriets, T., et al., *The macrosphere model: evaluation of a new stroke model for permanent middle cerebral artery occlusion in rats.* Journal of neuroscience methods, 2003. **122**(2): p. 201-211.
153. Zhang, Z., et al., *A new rat model of thrombotic focal cerebral ischemia.* Journal of Cerebral Blood Flow & Metabolism, 1997. **17**(2): p. 123-135.
154. Orset, C., et al., *Mouse model of in situ thromboembolic stroke and reperfusion.* Stroke, 2007. **38**(10): p. 2771-2778.
155. Ansar, S., et al., *Characterization of a new model of thromboembolic stroke in C57 black/6J mice.* Translational stroke research, 2014. **5**(4): p. 526-533.
156. Overgaard, K., *Thrombolytic therapy in experimental embolic stroke.* Cerebrovascular and brain metabolism reviews, 1994. **6**(3): p. 257-286.
157. Zhang, L., et al., *Intravenous Administration of a GPIIb/IIIa Receptor Antagonist Extends the Therapeutic Window of Intra-Arterial Tenecteplase–Tissue Plasminogen Activator in a Rat Stroke Model.* Stroke, 2004. **35**(12): p. 2890-2895.
158. Ren, M., et al., *Embolic middle cerebral artery occlusion model using thrombin and fibrinogen composed clots in rat.* Journal of neuroscience methods, 2012. **211**(2): p. 296-304.
159. Beech, J.S., et al., *Further characterisation of a thromboembolic model of stroke in the rat.* Brain research, 2001. **895**(1-2): p. 18-24.
160. Niessen, F., et al., *Differences in clot preparation determine outcome of recombinant tissue plasminogen activator treatment in experimental thromboembolic stroke.* Stroke, 2003. **34**(8): p. 2019-2024.
161. Tian, W., et al., *Hyaluronic acid hydrogel as Nogo-66 receptor antibody delivery system for the repairing of injured rat brain: in vitro.* Journal of Controlled Release, 2005. **102**(1): p. 13-22.
162. Malafaya, P.B., G.A. Silva, and R.L. Reis, *Natural–origin polymers as carriers and scaffolds for biomolecules and cell delivery in tissue engineering applications.* Advanced drug delivery reviews, 2007. **59**(4-5): p. 207-233.
163. Johnson, P.J., et al., *Controlled release of neurotrophin-3 and platelet-derived growth factor from fibrin scaffolds containing neural progenitor cells enhances survival and differentiation into neurons in a subacute model of SCI.* Cell transplantation, 2010. **19**(1): p. 89-101.
164. Yang, Z., et al., *The effect of the dosage of NT-3/chitosan carriers on the proliferation and differentiation of neural stem cells.* Biomaterials, 2010. **31**(18): p. 4846-4854.
165. Cooke, M.J., et al., *Controlled epi-cortical delivery of epidermal growth factor for the stimulation of endogenous neural stem cell proliferation in stroke-injured brain.* Biomaterials, 2011. **32**(24): p. 5688-5697.

166. Wang, Y., et al., *Combination of hyaluronic acid hydrogel scaffold and PLGA microspheres for supporting survival of neural stem cells.* Pharmaceutical research, 2011. **28**(6): p. 1406.
167. Austin, J.W., et al., *The effects of intrathecal injection of a hyaluronan-based hydrogel on inflammation, scarring and neurobehavioural outcomes in a rat model of severe spinal cord injury associated with arachnoiditis.* Biomaterials, 2012. **33**(18): p. 4555-4564.
168. Mittapalli, R.K., et al., *Paclitaxel–hyaluronic nanoconjugates prolong overall survival in a preclinical brain metastases of breast cancer model.* Molecular cancer therapeutics, 2013. **12**(11): p. 2389-2399.
169. Khaing, Z.Z., et al., *Advanced biomaterials for repairing the nervous system: what can hydrogels do for the brain?* Materials Today, 2014. **17**(7): p. 332-340.
170. Machova Urdzikova, L., et al., *The anti-inflammatory compound curcumin enhances locomotor and sensory recovery after spinal cord injury in rats by immunomodulation.* International journal of molecular sciences, 2016. **17**(1): p. 49.
171. Moshayedi, P., et al., *Systematic optimization of an engineered hydrogel allows for selective control of human neural stem cell survival and differentiation after transplantation in the stroke brain.* Biomaterials, 2016. **105**: p. 145-155.
172. Yao, S., et al., *Directing neural stem cell fate with biomaterial parameters for injured brain regeneration.* Progress in Natural Science: Materials International, 2013. **23**(2): p. 103-112.
173. Jiazhi, Y., et al., *Antibacterial properties of novel bacterial cellulose nanofiber containing silver nanoparticles.* Chinese Journal of Chemical Engineering, 2013. **21**(12): p. 1419-1424.
174. Czaja, W.K., et al., *The future prospects of microbial cellulose in biomedical applications.* biomacromolecules, 2007. **8**(1): p. 1-12.
175. El-Saied, H., A.H. Basta, and R.H. Gobran, *Research progress in friendly environmental technology for the production of cellulose products (bacterial cellulose and its application).* Polymer-Plastics Technology and Engineering, 2004. **43**(3): p. 797-820.
176. Jozala, A.F., et al., *Bacterial cellulose production by Gluconacetobacter xylinus by employing alternative culture media.* Applied microbiology and biotechnology, 2015. **99**(3): p. 1181-1190.
177. Ji, K., et al., *Bacterial cellulose synthesis mechanism of facultative anaerobe Enterobacter sp. FY-07.* Scientific reports, 2016. **6**: p. 21863.
178. Klemm, D., et al., *Bacterial synthesized cellulose—artificial blood vessels for microsurgery.* Progress in polymer science, 2001. **26**(9): p. 1561-1603.
179. Gea, S., et al., *Investigation into the structural, morphological, mechanical and thermal behaviour of bacterial cellulose after a two-step purification process.* Bioresource technology, 2011. **102**(19): p. 9105-9110.
180. Meftahi, A., et al., *Effect of Purification on Nano Microbial Cellulose Pellicle Properties.* Procedia Materials Science, 2015. **11**: p. 206-211.
181. McKenna, B.A., et al., *Mechanical and structural properties of native and alkali-treated bacterial cellulose produced by Gluconacetobacter xylinus strain ATCC 53524.* Cellulose, 2009. **16**(6): p. 1047.
182. Barud, H.S., et al., *Bacterial cellulose/poly (3-hydroxybutyrate) composite membranes.* Carbohydrate Polymers, 2011. **83**(3): p. 1279-1284.

183. Xu, C., et al., *Bacterial cellulose membranes used as artificial substitutes for dural defection in rabbits.* International journal of molecular sciences, 2014. **15**(6): p. 10855-10867.
184. Lin, S.-B., et al., *Adding enzymatically modified gelatin to enhance the rehydration abilities and mechanical properties of bacterial cellulose.* Food hydrocolloids, 2009. **23**(8): p. 2195-2203.
185. Yan, Z., et al., *Cellulose synthesized by Acetobacter xylinum in the presence of multi-walled carbon nanotubes.* Carbohydrate Research, 2008. **343**(1): p. 73-80.
186. Shah, N., et al., *Overview of bacterial cellulose composites: a multipurpose advanced material.* Carbohydrate Polymers, 2013. **98**(2): p. 1585-1598.
187. Recouvreux, D.O., et al., *Novel three-dimensional cocoon-like hydrogels for soft tissue regeneration.* Materials Science and Engineering: C, 2011. **31**(2): p. 151-157.
188. Cheng, K.-C., J.M. Catchmark, and A. Demirci, *Effect of different additives on bacterial cellulose production by Acetobacter xylinum and analysis of material property.* Cellulose, 2009. **16**(6): p. 1033.
189. Shezad, O., et al., *Physicochemical and mechanical characterization of bacterial cellulose produced with an excellent productivity in static conditions using a simple fed-batch cultivation strategy.* Carbohydrate Polymers, 2010. **82**(1): p. 173-180.
190. Bäckdahl, H., et al., *Mechanical properties of bacterial cellulose and interactions with smooth muscle cells.* Biomaterials, 2006. **27**(9): p. 2141-2149.
191. Camarero, J., et al. *A New Method for the Preparation of Peptide C-Terminal a-Thioesters Compatible with Fmoc-Solid-Phase Peptide Synthesis*. in *PEPTIDES-AMERICAN SYMPOSIUM*-. 2004. Kluwer Academic Publishers.
192. Berti, F.V., et al., *Nanofiber density determines endothelial cell behavior on hydrogel matrix.* Materials Science and Engineering: C, 2013. **33**(8): p. 4684-4691.
193. Klemm, D., et al., *Cellulose: fascinating biopolymer and sustainable raw material.* Angewandte Chemie International Edition, 2005. **44**(22): p. 3358-3393.
194. Zang, S., et al., *Study of osteogenic differentiation of human adipose-derived stem cells (HASCs) on bacterial cellulose.* Carbohydrate polymers, 2014. **104**: p. 158-165.
195. Helenius, G., et al., *In vivo biocompatibility of bacterial cellulose.* Journal of Biomedical Materials Research Part A: An Official Journal of The Society for Biomaterials, The Japanese Society for Biomaterials, and The Australian Society for Biomaterials and the Korean Society for Biomaterials, 2006. **76**(2): p. 431-438.
196. Zhu, C., et al., *Kombucha-synthesized bacterial cellulose: Preparation, characterization, and biocompatibility evaluation.* Journal of Biomedical Materials Research Part A, 2014. **102**(5): p. 1548-1557.
197. Scherner, M., et al., *In vivo application of tissue-engineered blood vessels of bacterial cellulose as small arterial substitutes: proof of concept?* journal of surgical research, 2014. **189**(2): p. 340-347.
198. Kwak, M.H., et al., *Bacterial cellulose membrane produced by Acetobacter sp. A10 for burn wound dressing applications.* Carbohydrate polymers, 2015. **122**: p. 387-398.
199. Katepetch, C., R. Rujiravanit, and H. Tamura, *Formation of nanocrystalline ZnO particles into bacterial cellulose pellicle by ultrasonic-assisted in situ synthesis.* Cellulose, 2013. **20**(3): p. 1275-1292.
200. Meftahi, A., et al., *The effects of cotton gauze coating with microbial cellulose.* Cellulose, 2010. **17**(1): p. 199-204.

201. Wei, B., G. Yang, and F. Hong, *Preparation and evaluation of a kind of bacterial cellulose dry films with antibacterial properties.* Carbohydrate Polymers, 2011. **84**(1): p. 533-538.
202. Barud, H.S., et al., *Antimicrobial bacterial cellulose-silver nanoparticles composite membranes.* Journal of Nanomaterials, 2011. **2011**: p. 10.
203. Saibuatong, O.-a. and M. Phisalaphong, *Novo aloe vera–bacterial cellulose composite film from biosynthesis.* Carbohydrate Polymers, 2010. **79**(2): p. 455-460.
204. Millon, L.E., G. Guhados, and W. Wan, *Anisotropic polyvinyl alcohol—Bacterial cellulose nanocomposite for biomedical applications.* Journal of Biomedical Materials Research Part B: Applied Biomaterials: An Official Journal of The Society for Biomaterials, The Japanese Society for Biomaterials, and The Australian Society for Biomaterials and the Korean Society for Biomaterials, 2008. **86**(2): p. 444-452.
205. Wang, J., Y. Wan, and Y. Huang, *Immobilisation of heparin on bacterial cellulose-chitosan nano-fibres surfaces via the cross-linking technique.* IET nanobiotechnology, 2012. **6**(2): p. 52-57.
206. Svensson, A., et al., *Bacterial cellulose as a potential scaffold for tissue engineering of cartilage.* Biomaterials, 2005. **26**(4): p. 419-431.
207. Feldmann, E.-M., et al., *Description of a novel approach to engineer cartilage with porous bacterial nanocellulose for reconstruction of a human auricle.* Journal of biomaterials applications, 2013. **28**(4): p. 626-640.
208. Nimeskern, L., et al., *Mechanical evaluation of bacterial nanocellulose as an implant material for ear cartilage replacement.* Journal of the mechanical behavior of biomedical materials, 2013. **22**: p. 12-21.
209. Bodin, A., et al., *Bacterial cellulose as a potential meniscus implant.* Journal of tissue engineering and regenerative medicine, 2007. **1**(5): p. 406-408.
210. Saska, S., et al., *Bacterial cellulose-hydroxyapatite nanocomposites for bone regeneration.* International journal of biomaterials, 2011. **2011**.
211. Shi, Q., et al., *The osteogenesis of bacterial cellulose scaffold loaded with bone morphogenetic protein-2.* Biomaterials, 2012. **33**(28): p. 6644-6649.
212. Zaborowska, M., et al., *Microporous bacterial cellulose as a potential scaffold for bone regeneration.* Acta biomaterialia, 2010. **6**(7): p. 2540-2547.
213. Mori, R., et al., *Increased antibiotic release from a bone cement containing bacterial cellulose.* Clinical Orthopaedics and Related Research®, 2011. **469**(2): p. 600-606.
214. Ran, J., et al., *Constructing multi-component organic/inorganic composite bacterial cellulose-gelatin/hydroxyapatite double-network scaffold platform for stem cell-mediated bone tissue engineering.* Materials Science and Engineering: C, 2017. **78**: p. 130-140.
215. Yoshino, A., et al., *Applicability of bacterial cellulose as an alternative to paper points in endodontic treatment.* Acta biomaterialia, 2013. **9**(4): p. 6116-6122.
216. Voicu, G., et al., *Improvement of silicate cement properties with bacterial cellulose powder addition for applications in dentistry.* Carbohydrate polymers, 2017. **174**: p. 160-170.
217. Huang, L., et al., *Nano-cellulose 3D-networks as controlled-release drug carriers.* Journal of Materials Chemistry B, 2013. **1**(23): p. 2976-2984.
218. Amin, M., et al., *Bacterial cellulose film coating as drug delivery system: physicochemical, thermal and drug release properties.* Sains Malaysiana, 2012. **41**(5): p. 561-568.
219. Bouet, V., et al., *The adhesive removal test: a sensitive method to assess sensorimotor deficits in mice.* Nature protocols, 2009. **4**(10): p. 1560.

220. Freret, T., et al., *Behavioral deficits after distal focal cerebral ischemia in mice: Usefulness of adhesive removal test.* Behavioral neuroscience, 2009. **123**(1): p. 224.
221. Montoya, C., et al., *The "staircase test": a measure of independent forelimb reaching and grasping abilities in rats.* Journal of neuroscience methods, 1991. **36**(2-3): p. 219-228.
222. Colbourne, F., et al., *Prolonged but delayed postischemic hypothermia: a long-term outcome study in the rat middle cerebral artery occlusion model.* Journal of Cerebral Blood Flow & Metabolism, 2000. **20**(12): p. 1702-1708.
223. Feeney, D.M., et al., *Responses to cortical injury: I. Methodology and local effects of contusions in the rat.* Brain research, 1981. **211**(1): p. 67-77.
224. Erdő, F., et al., *Talampanel improves the functional deficit after transient focal cerebral ischemia in rats. A 30-day follow up study.* Brain research bulletin, 2006. **68**(4): p. 269-276.
225. Zhang, L., et al., *A test for detecting long-term sensorimotor dysfunction in the mouse after focal cerebral ischemia.* Journal of neuroscience methods, 2002. **117**(2): p. 207-214.
226. Schallert, T., *Behavioral tests for preclinical intervention assessment.* NeuroRx, 2006. **3**(4): p. 497-504.
227. Markgraf, C.G., et al., *Sensorimotor and cognitive consequences of middle cerebral artery occlusion in rats.* Brain research, 1992. **575**(2): p. 238-246.
228. Li, J., et al., *The pre-ischaemic neuroprotective effects of the polyamine analogues BU43b and BU36b in permanent and transient focal cerebral ischaemia models in mice.* Brain research, 2006. **1076**(1): p. 209-215.
229. Ji, H.-J., et al., *Neuroprotective effects of the novel polyethylene glycol-hemoglobin conjugate SB1 on experimental cerebral thromboembolism in rats.* European journal of pharmacology, 2007. **566**(1-3): p. 83-87.
230. Wang, S., et al., *Anhedonia and activity deficits in rats: impact of post-stroke depression.* Journal of psychopharmacology, 2009. **23**(3): p. 295-304.
231. Ishibashi, S., et al., *Neurological dysfunctions versus regional infarction volume after focal ischemia in Mongolian gerbils.* Stroke, 2003. **34**(6): p. 1501-1506.
232. Vendrame, M., et al., *Infusion of human umbilical cord blood cells in a rat model of stroke dose-dependently rescues behavioral deficits and reduces infarct volume.* Stroke, 2004. **35**(10): p. 2390-2395.
233. Takahashi, K., et al., *Embryonic neural stem cells transplanted in middle cerebral artery occlusion model of rats demonstrated potent therapeutic effects, compared to adult neural stem cells.* Brain research, 2008. **1234**: p. 172-182.
234. Tennant, K.A. and T.A. Jones, *Sensorimotor behavioral effects of endothelin-1 induced small cortical infarcts in C57BL/6 mice.* Journal of neuroscience methods, 2009. **181**(1): p. 18-26.
235. Yager, J.Y., et al., *The influence of aging on recovery following ischemic brain damage.* Behavioural brain research, 2006. **173**(2): p. 171-180.
236. Fang, P.-c., et al., *Combination of NEP 1-40 treatment and motor training enhances behavioral recovery after a focal cortical infarct in rats.* Stroke, 2010. **41**(3): p. 544-549.
237. Hodges, H., *Maze procedures: the radial-arm and water maze compared.* Cognitive Brain Research, 1996. **3**(3-4): p. 167-181.
238. Choi, S.H., et al., *A simple modification of the water maze test to enhance daily detection of spatial memory in rats and mice.* Journal of Neuroscience Methods, 2006. **156**(1-2): p. 182-193.

239. Borlongan, C.V., et al., *Central nervous system entry of peripherally injected umbilical cord blood cells is not required for neuroprotection in stroke.* Stroke, 2004. **35**(10): p. 2385-2389.
240. Bouët, V., et al., *Sensorimotor and cognitive deficits after transient middle cerebral artery occlusion in the mouse.* Experimental neurology, 2007. **203**(2): p. 555-567.
241. Chen, J., et al., *Therapeutic benefit of intravenous administration of bone marrow stromal cells after cerebral ischemia in rats.* Stroke, 2001. **32**(4): p. 1005-1011.
242. Ma, M., et al., *Intranasal delivery of transforming growth factor-beta1 in mice after stroke reduces infarct volume and increases neurogenesis in the subventricular zone.* BMC neuroscience, 2008. **9**(1): p. 117.
243. Bederson, J.B., et al., *Rat middle cerebral artery occlusion: evaluation of the model and development of a neurologic examination.* stroke, 1986. **17**(3): p. 472-476.
244. Li, Y., et al., *Treatment of stroke in rat with intracarotid administration of marrow stromal cells.* Neurology, 2001. **56**(12): p. 1666-1672.
245. Freret, T., et al., *Delayed administration of deferoxamine reduces brain damage and promotes functional recovery after transient focal cerebral ischemia in the rat.* European Journal of Neuroscience, 2006. **23**(7): p. 1757-1765.
246. Yonemori, F., et al., *Spatial memory disturbance after focal cerebral ischemia in rats.* Journal of Cerebral Blood Flow & Metabolism, 1996. **16**(5): p. 973-980.
247. Chen, J., et al., *Intravenous administration of human umbilical cord blood reduces behavioral deficits after stroke in rats.* Stroke, 2001. **32**(11): p. 2682-2688.
248. Obana, W.G., L.H. Pitts, and M.C. Nishimura, *Effect of opiate antagonists on middle cerebral artery occlusion infarct in the rat.* Journal of neurosurgery, 1988. **69**(1): p. 98-103.
249. Chen, J., et al., *Atorvastatin induction of VEGF and BDNF promotes brain plasticity after stroke in mice.* Journal of cerebral blood flow & Metabolism, 2005. **25**(2): p. 281-290.
250. Gharbawie, O.A., P.A. Whishaw, and I.Q. Whishaw, *The topography of three-dimensional exploration: a new quantification of vertical and horizontal exploration, postural support, and exploratory bouts in the cylinder test.* Behavioural brain research, 2004. **151**(1-2): p. 125-135.
251. Schallert, T., et al., *CNS plasticity and assessment of forelimb sensorimotor outcome in unilateral rat models of stroke, cortical ablation, parkinsonism and spinal cord injury.* neuropharmacology, 2000. **39**(5): p. 777-787.
252. Bland, S.T., et al., *Early exclusive use of the affected forelimb after moderate transient focal ischemia in rats.* Stroke, 2000. **31**(5): p. 1144-1152.
253. Schallert, T., et al., *Tactile extinction: distinguishing between sensorimotor and motor asymmetries in rats with unilateral nigrostriatal damage.* Pharmacology Biochemistry and Behavior, 1982. **16**(3): p. 455-462.
254. Schallert, T. and M.T. Woodlee, *Orienting and placing.* The behavior of the laboratory rat: A handbook with tests, 2005: p. 129-140.
255. Hua, Y., et al., *Behavioral tests after intracerebral hemorrhage in the rat.* Stroke, 2002. **33**(10): p. 2478-2484.
256. Clarke, J., et al., *The effects of repeated rehabilitation "tune-ups" on functional recovery after focal ischemia in rats.* Neurorehabilitation and neural repair, 2009. **23**(9): p. 886-894.

257. Hurtado, O., et al., *A chronic treatment with CDP-choline improves functional recovery and increases neuronal plasticity after experimental stroke.* Neurobiology of disease, 2007. **26**(1): p. 105-111.
258. Machado, A.G., et al., *Chronic electrical stimulation of the contralesional lateral cerebellar nucleus enhances recovery of motor function after cerebral ischemia in rats.* Brain research, 2009. **1280**: p. 107-116.
259. Wakayama, K., et al., *Quantitative measurement of neurological deficit after mild (30 min) transient middle cerebral artery occlusion in rats.* Brain research, 2007. **1130**: p. 181-187.
260. Hrnkova, M., et al., *Neurodegeneration caused by expression of human truncated tau leads to progressive neurobehavioural impairment in transgenic rats.* Brain research, 2007. **1130**: p. 206-213.
261. Schallert, T., M. Woodlee, and S. Fleming, *Disentangling multiple types of recovery from brain injury.* Pharmacology of cerebral ischemia, 2002. **2002**: p. 201-216.
262. Kleim, J.A., J.A. Boychuk, and D.L. Adkins, *Rat models of upper extremity impairment in stroke.* ILAR journal, 2007. **48**(4): p. 374-385.
263. Urakawa, S., et al., *Environmental enrichment brings a beneficial effect on beam walking and enhances the migration of doublecortin-positive cells following striatal lesions in rats.* Neuroscience, 2007. **144**(3): p. 920-933.
264. Metz, G.A. and I.Q. Whishaw, *Cortical and subcortical lesions impair skilled walking in the ladder rung walking test: a new task to evaluate fore-and hindlimb stepping, placing, and co-ordination.* Journal of neuroscience methods, 2002. **115**(2): p. 169-179.
265. Farr, T.D., et al., *Bilateral alteration in stepping pattern after unilateral motor cortex injury: a new test strategy for analysis of skilled limb movements in neurological mouse models.* Journal of neuroscience methods, 2006. **153**(1): p. 104-113.
266. Rosen, C.L., et al., *Results of the prospective, randomized, multicenter clinical trial evaluating a biosynthesized cellulose graft for repair of dural defects.* Neurosurgery, 2011. **69**(5): p. 1093-1104.
267. Caroli, E., et al., *Duraplasty: our current experience.* Surgical neurology, 2004. **61**(1): p. 55-59.
268. Malliti, M., et al., *Comparison of deep wound infection rates using a synthetic dural substitute (neuro-patch) or pericranium graft for dural closure: a clinical review of 1 year.* Neurosurgery, 2004. **54**(3): p. 599-604.
269. Laquerriere, A., et al., *Experimental evaluation of bilayered human collagen as a dural substitute.* Journal of neurosurgery, 1993. **78**(3): p. 487-491.
270. McCall, T.D., D.W. Fults, and R.H. Schmidt, *Use of resorbable collagen dural substitutes in the presence of cranial and spinal infections—report of 3 cases.* Surgical neurology, 2008. **70**(1): p. 92-96.
271. Tachibana, E., et al., *Evaluation of the healing process after dural reconstruction achieved using a free fascial graft.* Journal of neurosurgery, 2002. **96**(2): p. 280-286.
272. Azzam, D., et al., *Dural repair in cranial surgery is associated with moderate rates of complications with both autologous and nonautologous dural substitutes.* World neurosurgery, 2018. **113**: p. 244-248.
273. Hoover, D.A. and A. Mahmood, *Ossification of autologous pericranium used in duraplasty: Case report.* Journal of neurosurgery, 2001. **95**(2): p. 350-352.
274. Yamada, K., et al., *Development of a dural substitute from synthetic bioabsorbable polymers.* Journal of neurosurgery, 1997. **86**(6): p. 1012-1017.

275. Keller, J.T., et al., *The fate of autogenous grafts to the spinal dura: an experimental study.* Journal of neurosurgery, 1978. **49**(3): p. 412-418.
276. Lam, F.C. and E. Kasper, *Augmented autologous pericranium duraplasty in 100 posterior fossa surgeries—a retrospective case series.* Operative Neurosurgery, 2012. **71**(suppl_2): p. ons302-ons307.
277. Abla, A.A., et al., *Comparison of dural grafts in Chiari decompression surgery: review of the literature.* Journal of Craniovertebral Junction and Spine, 2010. **1**(1): p. 29.
278. Macfarlane, M. and L. Symon, *Lyophilised dura mater: experimental implantation and extended clinical neurosurgical use.* Journal of Neurology, Neurosurgery & Psychiatry, 1979. **42**(9): p. 854-858.
279. Campbell, J., C. Bassett, and J. Robertson, *Clinical use of freeze-dried human dura mater.* Journal of neurosurgery, 1958. **15**(2): p. 207-214.
280. Narotam, P.K., J.R. van Dellen, and K.D. Bhoola, *A clinicopathological study of collagen sponge as a dural graft in neurosurgery.* Journal of neurosurgery, 1995. **82**(3): p. 406-412.
281. von Wild, K.R., *Examination of the safety and efficacy of an absorbable dura mater substitute (Dura Patch®) in normal applications in neurosurgery.* Surgical neurology, 1999. **52**(4): p. 418-425.
282. Tomita, T., et al., *New dried human amniotic membrane is useful as a substitute for dural repair after skull base surgery.* Journal of Neurological Surgery Part B: Skull Base, 2012. **73**(05): p. 302-307.
283. Brzezicki, G., et al., *Evaluation of epidural scar formation in lumbar spine after TachoComb application-an experimental study.* Neurologia i neurochirurgia polska, 2008. **42**(3): p. 223-230.
284. Bejjani, G.K. and J. Zabramski, *Safety and efficacy of the porcine small intestinal submucosa dural substitute: results of a prospective multicenter study and literature review.* Journal of neurosurgery, 2007. **106**(6): p. 1028-1033.
285. Achilli, M. and D. Mantovani, *Tailoring mechanical properties of collagen-based scaffolds for vascular tissue engineering: the effects of pH, temperature and ionic strength on gelation.* Polymers, 2010. **2**(4): p. 664-680.
286. Moskowitz, S.I., J. Liu, and A.A. Krishnaney, *Postoperative complications associated with dural substitutes in suboccipital craniotomies.* Operative Neurosurgery, 2009. **64**(suppl_1): p. ONS28-ONS34.
287. Bowers, C.A., et al., *AlloDerm for duraplasty in Chiari malformation: superior outcomes.* Acta neurochirurgica, 2015. **157**(3): p. 507-511.
288. Martínez-Lage, J.F., et al., *Autologous tissues for dural grafting in children: a report of 56 cases.* Child's Nervous System, 2006. **22**(2): p. 139-144.
289. Martínez-Lage, J.F., et al., *Creutzfeldt-Jakob disease acquired via a dural graft: failure of therapy with quinacrine and chlorpromazine.* Surgical neurology, 2005. **64**(6): p. 542-545.
290. Montinaro, A., C. Gianfreda, and P. Proto, *Equine pericardium for dural grafts: clinical results in 200 patients.* cell, 2007. **338**: p. 6406076.
291. Foy, A.B., C. Giannini, and C. Raffel, *Allergic reaction to a bovine dural substitute following spinal cord untethering: Case report.* Journal of Neurosurgery: Pediatrics, 2008. **1**(2): p. 167-169.
292. Esposito, F., et al., *Collagen-only biomatrix as a novel dural substitute: examination of the efficacy, safety and outcome: clinical experience on a series of 208 patients.* Clinical neurology and neurosurgery, 2008. **110**(4): p. 343-351.

293. Sommerich, B., et al., *In Vivo Tissue Reaction, Resorption, Safety, and Efficacy of a Collagen Dural Substitute in an Animal Model.* 2005.
294. Shi, Z., et al., *A new absorbable synthetic substitute with biomimetic design for dural tissue repair.* Artificial organs, 2016. **40**(4): p. 403-413.
295. Kundu, B., et al., *Silk fibroin biomaterials for tissue regenerations.* Advanced drug delivery reviews, 2013. **65**(4): p. 457-470.
296. Kim, D.W., et al., *A transparent artificial dura mater made of silk fibroin as an inhibitor of inflammation in craniotomized rats.* Journal of neurosurgery, 2011. **114**(2): p. 485-490.
297. Sherman, J.H., et al., *Reconstruction of the sellar dura in transsphenoidal surgery using an expanded polytetrafluoroethylene dural substitute.* Surgical neurology, 2008. **69**(1): p. 73-76.
298. KAWAGUCHI, T., et al., *Expanded polytetrafluoroethylene membrane for prevention of adhesions in patients undergoing external decompression and subsequent cranioplasty.* Neurologia medico-chirurgica, 2003. **43**(6): p. 320-324.
299. Vakis, A., et al., *Use of polytetrafluoroethylene dural substitute as adhesion preventive material during craniectomies.* Clinical neurology and neurosurgery, 2006. **108**(8): p. 798-802.
300. Otailo, S. and M. Sacks. *Mechanical Behavior of Human Dura Mater*. in *Proc. 1995 Bioengineering Conference*. 1995.
301. Sacks, M.S., et al., *Local mechanical anisotropy in human cranial dura mater allografts.* Journal of biomechanical engineering, 1998. **120**(4): p. 541-544.
302. Schramm, M. and S. Hestrin, *Factors affecting production of cellulose at the air/liquid interface of a culture of Acetobacter xylinum.* Microbiology, 1954. **11**(1): p. 123-129.
303. Fischer, A.H., et al., *Hematoxylin and eosin staining of tissue and cell sections.* Cold spring harbor protocols, 2008. **2008**(5): p. pdb. prot4986.
304. MacLellan, C.L., et al., *Gauging recovery after hemorrhagic stroke in rats: implications for cytoprotection studies.* Journal of Cerebral Blood Flow & Metabolism, 2006. **26**(8): p. 1031-1042.
305. Karthikeyan, S., et al., *Characterizing spontaneous motor recovery following cortical and subcortical stroke in the rat.* Neurorehabilitation and neural repair, 2019. **33**(1): p. 27-37.
306. Klein, A. and S.B. Dunnett, *Analysis of skilled forelimb movement in rats: the single pellet reaching test and staircase test.* Current protocols in neuroscience, 2012. **58**(1): p. 8.28. 1-8.28. 15.
307. Li, J. and D.J. Mooney, *Designing hydrogels for controlled drug delivery.* Nature Reviews Materials, 2016. **1**(12): p. 16071.
308. Varshosaz, J. and M. Hajian, *Characterization of drug release and diffusion mechanism through hydroxyethylmethacrylate/methacrylic acid pH-sensitive hydrogel.* Drug delivery, 2004. **11**(1): p. 53-58.
309. Schnieders, J., et al., *The effect of porosity on drug release kinetics from vancomycin microsphere/calcium phosphate cement composites.* Journal of Biomedical Materials Research Part B: Applied Biomaterials, 2011. **99**(2): p. 391-398.
310. Berjano, R., F.C. Vinas, and M. Dujovny, *A review of dural substitutes used in neurosurgery.* Critical Reviews in Neurosurgery, 1999. **9**(4): p. 217-222.
311. Danish, S.F., et al., *Experience with acellular human dura and bovine collagen matrix for duraplasty after posterior fossa decompression for Chiari malformations.* Journal of Neurosurgery: Pediatrics, 2006. **104**(1): p. 16-20.

312. Chen, S.-Q., et al., *Mechanical properties of bacterial cellulose synthesised by diverse strains of the genus Komagataeibacter.* Food hydrocolloids, 2018. **81**: p. 87-95.
313. De Kegel, D., et al., *Biomechanical characterization of human dura mater.* Journal of the mechanical behavior of biomedical materials, 2018. **79**: p. 122-134.
314. Ikeda, T., et al., *Limited differentiation to neurons and astroglia from neural stem cells in the cortex and striatum after ischemia/hypoxia in the neonatal rat brain.* American journal of obstetrics and gynecology, 2005. **193**(3): p. 849-856.
315. Modulevsky, D.J., C.M. Cuerrier, and A.E. Pelling, *Biocompatibility of subcutaneously implanted plant-derived cellulose biomaterials.* PloS one, 2016. **11**(6): p. e0157894.
316. DiResta, G.R., J. Lee, and E. Arbit, *Measurement of brain tissue specific gravity using pycnometry.* Journal of neuroscience methods, 1991. **39**(3): p. 245-251.
317. Kolb, B., et al., *Growth factor-stimulated generation of new cortical tissue and functional recovery after stroke damage to the motor cortex of rats.* Journal of cerebral blood flow & metabolism, 2007. **27**(5): p. 983-997.
318. Aravamudhan, A., et al., *Osteoinductive small molecules: growth factor alternatives for bone tissue engineering.* Current pharmaceutical design, 2013. **19**(19): p. 3420-3428.
319. Xiong, Y., A. Mahmood, and M. Chopp, *Emerging potential of exosomes for treatment of traumatic brain injury.* Neural regeneration research, 2017. **12**(1): p. 19.